Materials Today Bio 23 (2023) 100870

Contents lists available at ScienceDirect

Materials Today Bio

journal homepage: www.journals.elsevier.com/materials-today-bio

Recent advances in 3D bioprinted cartilage-mimicking constructs for applications in tissue engineering

Jian Zhou [a], Qi Li [a], Zhuang Tian [b], Qi Yao [b,*], Mingzhu Zhang [a,**]

[a] Department of Foot and Ankle Surgery, Beijing Tongren Hospital, Capital Medical University, Beijing, 100730, PR China
[b] Department of Joint Surgery, Beijing Shijitan Hospital, Capital Medical University, Beijing, 100038, PR China

ARTICLE INFO

Keywords:
Bioprinting
Cartilage
Bionics
Tissue engineering

ABSTRACT

Human cartilage tissue can be categorized into three types: hyaline cartilage, elastic cartilage and fibrocartilage. Each type of cartilage tissue possesses unique properties and functions, which presents a significant challenge for the regeneration and repair of damaged tissue. Bionics is a discipline in which humans study and imitate nature. A bionic strategy based on comprehensive knowledge of the anatomy and histology of human cartilage is expected to contribute to fundamental study of core elements of tissue repair. Moreover, as a novel tissue-engineered technology, 3D bioprinting has the distinctive advantage of the rapid and precise construction of targeted models. Thus, by selecting suitable materials, cells and cytokines, and by leveraging advanced printing technology and bionic concepts, it becomes possible to simultaneously realize multiple beneficial properties and achieve improved tissue repair. This article provides an overview of key elements involved in the combination of 3D bioprinting and bionic strategies, with a particular focus on recent advances in mimicking different types of cartilage tissue.

1. Introduction

The regeneration and repair of defective cartilage tissue has long been a challenge due to insufficient blood supply. Current therapeutic methods for cartilage diseases include artificial scaffolds [1,2], microfractures [3,4], autologous cartilage transplantation [5,6], stem cell therapy [7], and more [8]. While these operations have achieved some curative effects, they still have some problems, such as donor injury, long treatment cycles, prosthetic infection, and unsatisfactory curative efficacy. Advances in tissue engineering present a hopeful resolution to these problems. Tissue engineering involves applying both life science and engineering principles to create biological replacements that can repair damaged tissue. This process requires a comprehensive understanding of the specific physiological and pathological conditions of the targeted tissue. Various traditional techniques, such as lyophilization [9–11], electrospinning [12–14], injectable hydrogels [15–17], and microspheres [18,19], have been utilized in tissue engineering. With the rapid development of tissue-engineered technologies, supporting concepts have been consistently advanced. An optimal tissue-engineered scaffold must possess exceptional biocompatibility and chondrogenic ability, matching biodegradability, necessary porosity, and bionic shape, composition, histological structure and mechanics to accurately replicate damaged tissue [20]. Such a scaffold can not only replace damaged tissue quickly and delay the progression of lesions but also facilitate repair and regeneration processes.

As a novel tissue-engineered technology, 3D bioprinting offers the potential to create customized scaffolds with remarkable morphological precision. This technique provides natural advantages in simulating biological structures. By selecting suitable materials, cells, and cytokines and leveraging advanced printing technology and bionic concepts, it becomes possible to consider multiple properties simultaneously and achieve a higher level of biomimicry. This article provides an overview of key elements involved in 3D bioprinted cartilage-mimicking constructs (Fig. 1), with a particular focus on recent advances in mimicking different types of cartilage tissue.

2. Bionic orientations

In theory, tissues or organs can be considered composite structures made up of cells and extracellular matrix (ECM). These structures have

* Corresponding author.
** Corresponding author.
E-mail addresses: yqjh2010@163.com (Q. Yao), michaelzhang120@hotmail.com (M. Zhang).

https://doi.org/10.1016/j.mtbio.2023.100870
Received 7 July 2023; Received in revised form 10 November 2023; Accepted 14 November 2023
Available online 17 November 2023

evolved over millions of years to possess optimal properties for survival in nature. This serves as a crucial foundation for the implementation of biomimetic strategies in tissue engineering. The concept of bionics was first introduced by Steeles in 1960 [21], and in 1986, Hull [22] invented the first 3D printing technology known as stereolithography. Since then, the concept of bionic 3D printing has emerged. This technology is inspired by the principles of biological structure and function and is designed to create 3D printed structures with bionic properties. The concept of bionic 3D printing has evolved over time to satify the requirements of regenerative medicine. Currently, the directions of bionics mainly include morphological bionics, compositional bionics, mechanical bionics, and histological bionics.

In cartilage engineering, the functions of various cartilage tissues are diverse and rely on complex composition, unique shape, and reasonable histological structure. Additionally, their functionality is inseparable from the surrounding tissue. While 3D printing offers clear advantages in terms of morphological design, material and cell selection, and distribution, it still faces several challenges in achieving overall high-level biomimicry. Therefore, researchers often investigate different approaches to optimize the properties of printed constructs.

2.1. Composition

Composition is a key factor in distinguishing among different organizations. In cartilage, collagen and proteoglycans are the primary organic components, but the types and proportions of collagen can vary significantly across different types of cartilage. For instance, articular cartilage is composed of 80–90 % type II collagen, while type I collagen is virtually absent [23]. In contrast, the meniscus contains several types of collagen, with type I collagen being the most prevalent [24,25]. The composition of tissue not only determines its mechanical properties but also plays a crucial role in the microenvironment that enables cell survival. Extensive research has been conducted on the regulatory effect of tissue composition on cell behavior and tissue repair (Table 1).

Hyaluronic acid (HA) is an important component of cartilage, and its effect on cellular function was studied by Martiniac et al. [26]. Initially, they developed a new human chondrocyte Col2a1 Gaussian luciferase reporter system (HuCol2gLuc) that could detect the production of type II collagen noninvasively and with high throughput, enhancing the accuracy and convenience of the experiment. They subsequently compared the methacrylate (GelMA) group with the GelMA/hyaluronic acid methacrylate (HAMA) group and found that the addition of HAMA improved cartilage formation by 15 %.

With the most similar composition to native tissue, ECM has long been a research hotspot in tissue engineering. Some researchers [27] first explored the effects of different concentrations of ECM on cell behavior. In that study, five concentration gradients were designed: 0 %, 0.5 %, 1 %, 2 %, and 4 %. Following a 14-day culture *in vitro*, the 2 % group exhibited the highest levels of glycosaminoglycan (GAG) and collagen production. However, it is important to note that changes in concentration can often lead to variations in other physical properties of the hydrogel, including porosity, stiffness, swelling ratio, and the internal molecular network. The comparison of different materials is encounters similar problems as well. As a result, it is crucial to consider how to better control these variables to obtain more accurate results.

While the concept of compositional bionics for tissue repair is well understood, the natural materials used in this field are not easily printed. First, these materials essentially lack the necessary properties to be

Fig. 1. The core elements of bionic bioprinting for cartilage tissue engineering.

Table 1
Overview of componential bionic materials in different cartilage tissues.

The usual bionic materials	Merits	Demerits	Ref.
ECM	Closest composition to native tissue, excellent biocompatibility, good cell recruitment	High cost, unclear composition, unstable properties	33. 140. 147. 154.
Hyaluronic acid	Similar composition to native tissue, nontoxicity, good biocompatibility, optimization of cell function	Low viscosity, lack of gelation ability	26. 157.
Collgen	Similar composition to native tissue, low immunogenicity, optimization of cell behavior, good biological function	High cost, low mechanical strength	43. 156.
Silk Fibroin	Excellent mechanical strength, good biocompatibility, fine elasticity, low interfacial shear force	Lack of source and gelation ability	142. 184. 185.
GelMA	Low cost, stable properties, fast crosslinking, excellent printability, adjustable biodegradation	Unsatisfied biological function, fluctuated properties with varied temperature	60. 173. 175.
Alginate	Fast gelation kinetics, good shape fidelity	High immunogenicity, insufficient biocompatibility	160. 188.

printed as fluids, requiring complex processing or the addition of auxiliary materials. However, such procedures tend to compromise their initial physical properties and functionality. Additionally, challenges encountered during the printing process include inadequate homogeneity and unsuitable viscoelasticity. Therefore, it is imperative to address the issue of developing bionic materials that offer enhanced printing performance and satisfy the needs of compositional bionics.

2.2. Morphology

Morphology serves as an intuitive representation of organizational type and is a necessary condition for the realization of organizational functions. Unique shapes have evolved in various types of cartilage to fulfill their functional requirements. For instance, the auricle has a distinct shape that facilitates sound collection, while the trachea is designed to keep the airway open and facilitate constriction and relaxation. The wedge shape of the menisci allows a perfect fit between the femoral condyles and the tibial plateau for force transmission and load.

Furthermore, precise morphological bionics plays a crucial role in tissue repair, as depicted in Fig. 2. In particular, to repair articular cartilage defects, a well-shaped simulation is necessary for accurate scaffold implantation and subsequent restoration of alignment and stability. Vahdati et al. [28] conducted a study using the finite element method to examine the impact of adhesion between cartilage implants and native tissue. Larger implant sizes were shown to lead to a higher surface coefficient of friction and to increase the chance of implant loosening and delamination.

2.3. Histological structure

To meet functional demands, certain tissues display distinct orientations and zonal discrepancies in cell distribution and histological arrangement. These factors are crucial for optimizing tissue regeneration. The meniscus is a prime example of this relationship, as the inner and outer regions, posterior and anterior horns, and superficial and deep layers all exhibit diverse distributions of histological components [29]. Specifically, collagen fibers are arranged radially and circumferentially in different zones [30,31]. However, imitating such complex structures is an enormous challenge for researchers.

Bahcecioglu's research [32] initially focused on examining the histological differences between the inner and outer regions of the meniscus. To replicate the structure of the meniscus, a bionic scaffold made of polycaprolactone (PCL) in a coliseum shape was designed. Inner layer injection of agarose (Ag), GelMA, and meniscal fibrocartilage cells (MFCs) was performed, while the outer layer was perfused with GelMA + MFCs. Following six weeks of *in vitro* culture, cartilage-like tissue was observed in the inner layer and fibrocartilage-like tissue was observed in the outer layer, realizing the regeneration of differentiated structures. Guo et al. [33] addressed the anisotropic structure of the meniscus by simulating collagen assembly through 3D printing circular and radial PCL strands. They then infused ECM to achieve further componential mimicry. The resulting protection of articular cartilage and optimized meniscal regeneration were demonstrated in experimental models using rabbits and sheep.

A 3D printer may distribute and arrange materials in an organized fashion, but it falls short of reproducing the intricate details found in native tissue. Collagen fibers, for instance, are seamlessly connected in natural tissue, even at the nanoscale level. In contrast, at the macro level, 3D printed hydrogel strands exhibit a resolution of merely 100 μm [34,35] and retain numerous large pores, whereas at the micro level, the internal molecular assembly often lacks structural order. This fundamental flaw is responsible for the subpar mechanical properties of hydrogels, which fail to meet practical demands. Therefore, researchers often attempt to solve this problem by incorporating alternative materials. Nevertheless, even with these modifications, the microstructure of the resulting constructs still varies considerably from that of native tissue. Consequently, there is still a considerable gap to overcome to achieve fully biomimetic constructs.

2.4. Biomechanics

Cartilage tissue possesses unique mechanical properties, which are the basis of achieving its primary functions including shape retention, force transmission and cushioning. In the case of the human meniscus, its unique position and shape require strong mechanical strength and complex anisotropy. In detail, the axial compression modulus of the meniscus is approximately 100–150 kPa, while the shear modulus shows a similar strength of about 120 kPa. On the other hand, the tensile modulus far surpasses these values, reaching dozens of MPa in the radial direction and being 10 times higher in the circumferential direction [36]. These excellent mechanical properties harness their strengths in reducing the load on both the tibial platform and the femoral condyle [37]. Similarly, the articular cartilage also functions as a weight-bearing structure with an aggregate modulus of 1.8 MPa, contributing to its ability to withstand mechanical forces [38]. Additionally, the mechanical environment plays a crucial role in the behavior of chondrocytes and tissue regeneration [39]. Therefore, the development of bionic mechanical scaffolds is a highly researched topic in the field of 3D bioprinting.

A study by Martyniak et al. [26] explored the impact of scaffold stiffness on cartilage regeneration. By adjusting the ratio of GelMA and HAMA, researchers were able to create scaffolds with varying moduli of 32 kPa and 57.9 kPa. After 22 days in culture, it was discovered that rigid biomaterials showed higher expression of type II collagen with low mobility. A similar study was conducted by Michael et al. [40], who varied the ratio of alginate to chitosan to manipulate the mechanical properties of the hydrogel. This led to changes in cell behavior and further confirmed the significance of mechanics in tissue regeneration.

In addition to the inherent mechanical properties of the scaffold, external mechanical intervention plays a pivotal role in tissue repair. Chen et al. [41] developed an auxetic scaffold that incorporates 3D tensile stimulation to influence chondrocyte-seeded decellularized extracellular matrix (dECM) mixed with fish gelatin methacrylate

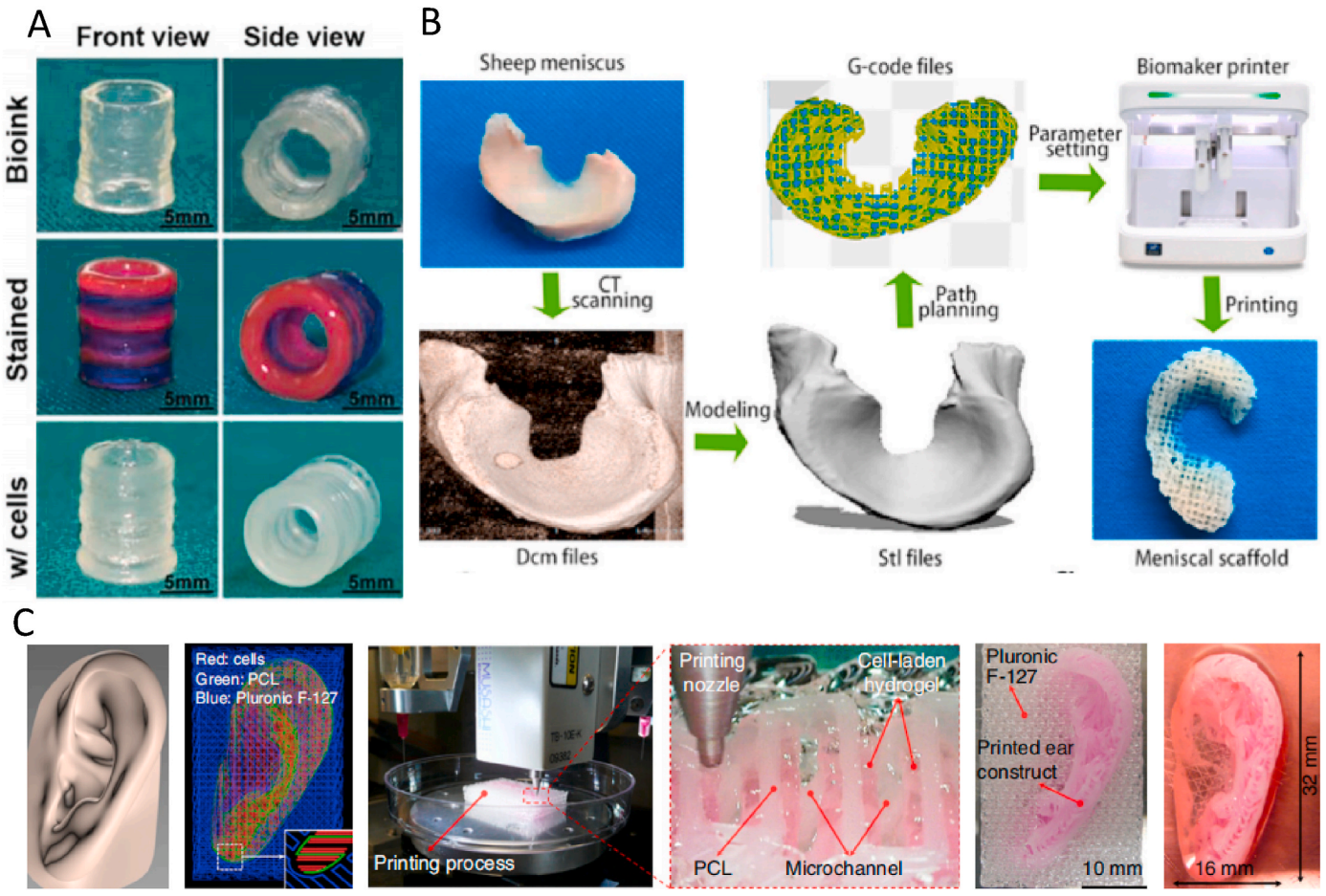

Fig. 2. Morphological mimicking scaffolds achieved by 3D bioprinting. (A) Pictures of the 3D printed tracheal construct without cells, the dye-stained tracheal construct, and the cell-laden tracheal construct [184]. (B) 3D bioprinting process of biomimetic meniscal scaffolds [60]. (C) 3D printing process of the biomimetic auricular scaffold [173].

(FGelMa) scaffold. The findings demonstrated that application of tensile force promotes the production of chondrogenesis-related markers, collagen II and glycosaminoglycans. Furthermore, they also confirmed that this process may be associated with the activation of yes-associated protein 1 signaling pathway.

2.5. Composite tissue

Because cartilage tissue lacks a blood supply, its survival and function depend on their bonds with surrounding tissue such as the trachea and mucous membranes, articular cartilage and subchondral bone, meniscus and synovial tissue. However, printing composite tissue requires careful consideration of numerous details. In addition to ensuring the necessary performance of each tissue, the design of composite tissue must also address various issues, such as interface connection, mechanical stability, and degradation coordination of different parts, which greatly increases the complexity of research. Nevertheless, the simultaneous construction of interconnected tissue could potentially serve as a shortcut for tissue or organ regeneration, but further research is required to validate this theory. At present, several researchers have conducted relevant studies on the 3D printing of composite tissue.

Zhou and colleagues [42] utilized stereolithography to create a biomimetic biphasic osteochondral construct (Fig. 3I). The upper layer consisted of GelMA and polyethylene glycol diacrylate (PEGDA)/-translational growth factor-β1 (TGF-β1), while the lower layer was made of GelMA-PEGDA/HA. The study found that the scaffold facilitated the differentiation of human mesenchymal stem cells (hMSCs) into osteogenic and chondrogenic lineages and upregulated genes associated with osteogenesis and chondrogenesis.

Bokey et al. [43] utilized the bionic concept in their tracheal bioprinting research as well. They developed a two-step printing approach to create a superior bionic tracheal scaffold. The first step involved printing the PCL bellows frame and enhancing its mechanical properties through heat and oxygen plasma treatment. In the second step, a single cartilage ring (3 % ectopic collagen bioink with human nasal chondrocytes (hNCCs)) and an epithelial layer (3 % ectopic collagen bioink with human nasal turbinate stem cells (hNTSCs)) were printed onto the outer groove and luminal surface of the bellows frame to achieve more realistic mimicry. Finally, a protective barrier, known as the PCL sinusoidal-patterned tubular mesh (SPTM), was incorporated into the outer layer of the scaffold to prevent rapid absorption of the cartilage ring after implantation (Fig. 3A–G). After 8 weeks of subcutaneous implantation in nude mice, a significant number of infiltrating microvessels were observed surrounding the regenerated cartilage, indicating successful fusion with the surrounding tissue. Simultaneously, histological staining revealed the formation of mature chondrocytes and cartilage-like extracellular matrix. This study successfully constructed a multilevel bionic trachea by combining 3D printing with various tissue-engineered techniques, achieving excellent outcomes in animal experiments through meticulous design.

2.6. Scaffold-free and cell-free strategies

Although the benefits of 3D bioprinted scaffolds are clear, it is important to acknowledge their drawbacks, including complex fabrication processes, high cost, the immunogenicity of natural materials and

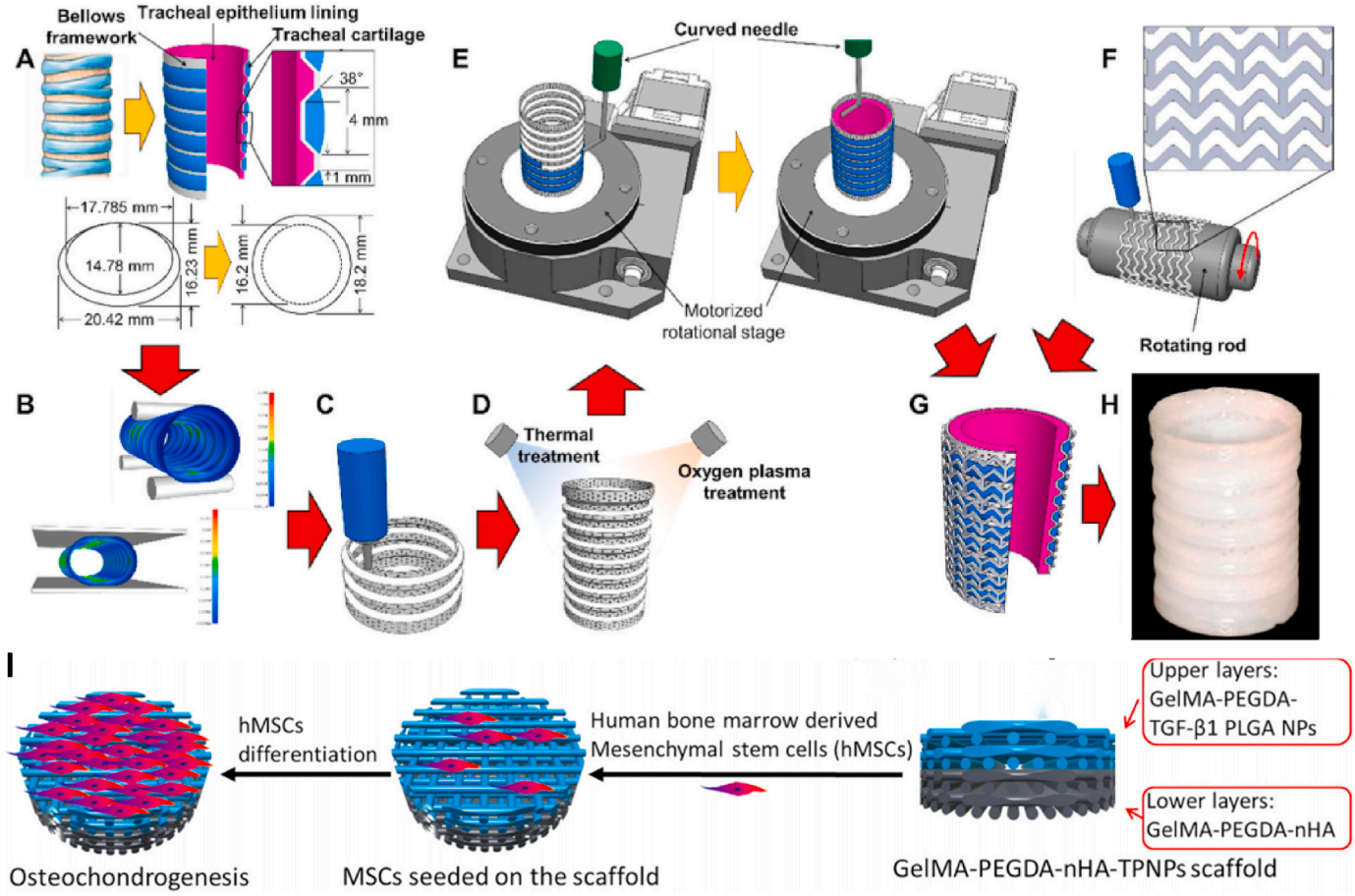

Fig. 3. Schematics of the trachea-mimetic scaffold [43] (A–G) and osteochondral scaffold [42] (I). Step 1: (A) The actual size of the construct. (B) The bellows framework. (C) The preparation of porosity in the bellows framework. (D) Thermal/oxygen plasma treatments. Step 2: (E) The preparation of cartilage rings and epithelial layer by rotary printing. (F) Preparation of a SPTM. (G) Diagram of the trachea-mimetic scaffold. (H) Image of the trachea-mimetic scaffold. (I) Schematics of hierarchical biomimetic osteochondral scaffold.

the toxicity of degradation byproducts in polymeric materials [44], which cannot currently be avoided. Additionally, finding a solution for the coordination between the degradation of the scaffold and the regeneration of neotissue is challenging. Moreover, the function of many 3D bioprinted scaffolds mainly depends on implanted or recruited cells, while the scaffold-free strategy directly taps the potential of cells and maximizes their value.

Ryusuke et al. [45] developed an elaborate layered, trachea-like, scaffold-free structure. They achieved this by coculturing chondrocytes, MSCs, and umbilical vein endothelial cells (HUVECs) to produce cartilage spheroids and normal human dermal fibroblasts (NHDFs), HUVECs, and MSCs to form neofibrous spheroids. Using the "Kenzan" method of 3D bioprinting, they successfully created a trachea-like construct. After maturation with the appropriate medium flow, the construct was implanted into a rat trachea defeat model. After 35 days in culture, histological staining revealed the development of large luminal structures, abundant GAGs, and type II collagen. In summary, scaffold-free strategies offer a wide range of cell options, but the cultivation of these cells necessitates a long-term commitment and a substantial quantity, thereby potentially requiring more stringent ethical scrutiny and posing clinical risks. Furthermore, the functions of various cells have not been systematically investigated.

In contrast, a cell-free strategy not only avoids the abovementioned issues but also allows for a focus on scaffold design and the recruitment of endogenous cells. Zhang et al. [46] utilized directional freezing technology to prepare silk fibroin scaffolds with horizontal and vertical arrangements and random porosity. The results demonstrated that this particular scaffold provided a more favorable microenvironment for endogenous bone marrow mesenchymal stem cells (BMSCs) than other scaffolds, promoting simultaneous regeneration of cartilage and subchondral bone. Additionally, Guo et al. [33] applied this strategy in systematic animal experiments, implanting 3D printed PCL-ECM scaffolds into meniscectomy models of rabbits and sheep. Knee magnetic resonance imaging (MRI) scanning revealed the presence of neomeniscal tissue in the experimental group, while Mankin scores indicated that the PCL-MECM scaffold effectively protected the articular cartilage. However, it remains to be determined whether the cell-free strategy can obtain sufficient endogenous cells, particularly in cartilage tissue.

3. Bionic bioprinting techniques

3D printing is a rapid manufacturing technology that builds 3D structures based on 3D model data. Bioprinting, by contrast, combines biological ink and the concepts of tissue engineering to construct biomimetic structures for repairing tissue defects. After decades of development, 3D bioprinting technology has been widely used in various medical fields [47–51] and has achieved promising results. Currently, the main techniques for bionic cartilage tissue include extrusion bioprinting, stereolithography and inkjet bioprinting (Table 2).

3.1. Extrusion bioprinting

Extrusion printing is a common manufacturing technology that involves extruding liquid ink onto a mobile platform through a syringe

Table 2
Overview of the characteristics of different bioprinting technologies.

Bioprinting techniques	Mterial demands	Resolution	Applied field	Advantages	Limitations	Ref.
Extrusion printing	High-viscosity liquild	Approximately 100 μm	Tissue-engineered scaffold, drug delivery, organoid	Suitable for large-scale and complex constructs, wide range of materials, support for multiple designs	Moderate precision and slow fabrication speed	52. 53.
Stereolithography	Photocrosslinked liquid	Approximately 10 μm	Regenerativemedicine	Fast printing, high cell viability	Restricted to photocrosslinking materials, high cost	64.
Inkjet printing	Low-viscosity liquid without impurities	Approximately 10 μm	Disease models, drug research	High precision, fast printing, low cost	Easily clogged nozzle, low cell density	66.

needle powered by either air pressure or a motor [52]. This method offers several advantages over other printing techniques, including a wide range of materials, fast printing speed, and high printing accuracy [53]. These advantages make extrusion printing particularly suitable for building large-scale structures in some fields such as cartilage, heart [54], bladder [55], muscles [56], bone [57,58] and kidney [59].

Bioinks used for extrusion printing require high viscosity to maintain their shape after printing, but this conflicts with the need for narrow syringe needles to improve printing resolution. As a result, two major challenges arise in concrete practice: cell viability and printability. To overcome these challenges, printing parameters must be adjusted and the rheological properties of the ink must be optimized. In their study, Zhou et al. [60] enhanced the printing capabilities of ECM by incorporating GelMA and utilizing sonication, resulting in improved shape accuracy during extrusion. In addition, by carefully adjusting the printing parameters and environmental conditions based on the rheological properties of the GelMA/ECM bioink, they were able to achieve a cell viability rate of over 95 % and produce highly precise scaffolds. Sakai et al. [61] investigated the impact of silk fibroin nanofibers on bioink printing properties (Fig. 4A). To obtain the nanofibers, they ground degummed silk fibers and added them to a polymer solution. The results showed a significant improvement in the shear-thinning properties of the ink, resulting in more precise and accurate structure building. Importantly, the addition of nanofibers did not have any adverse effects on cell viability or behavior.

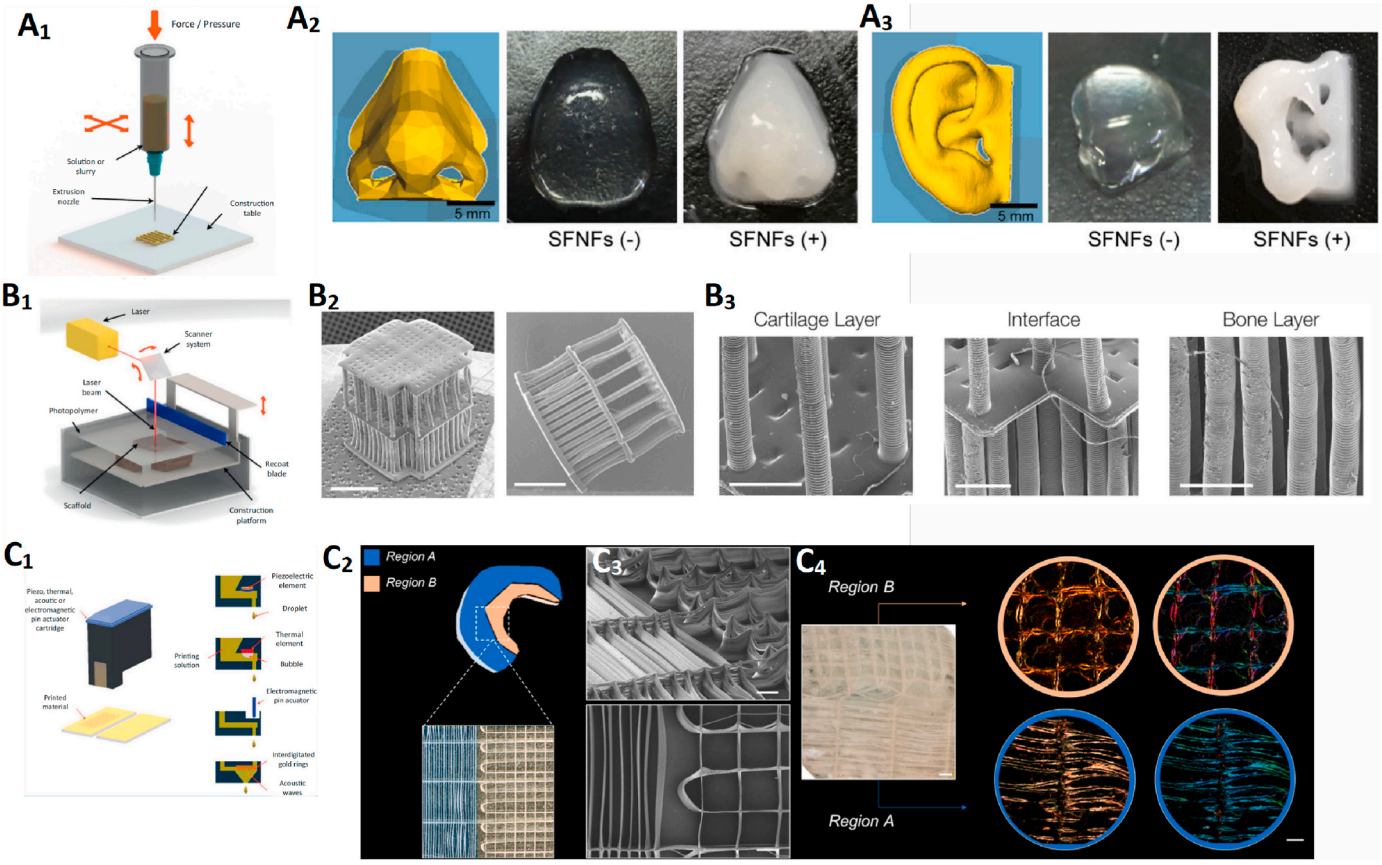

Fig. 4. Different types of bioprinting technologies and their applied scenarios. (A_1) Schematic diagram of extrusion bioprinting and its application in nose (A_2) and auricle (A_3) reconstruction [61]. Hydrogel with silk fibroin nanofibers (SFNFs+) and without silk fibroin nanofibers (SFNFs-). Schematic diagram of stereolithography (B_1) application in osteochondral composite tissue. Representative SEM images of the 3D printed bilayer. Full structure (B_2, scale bar = 2 mm). Close-up (B_3, scale bar = 500 μm) [65]. Schematic diagram of inkjet bioprinting (C_1) and its application in meniscus. Regionally distinct architectures constructed by MEW and inkjet bioprinting. (C_2) Schematic diagram and the designed scaffold. (C_3) SEM images (scale bar = 500 μm). (C_4) Bright field image (scale bar = 800 μm) of the scaffold after 4 weeks of *in vitro* culture and polarized light and color map imaging of the collagen fiber distributions (scale bar = 400 μm) [68].

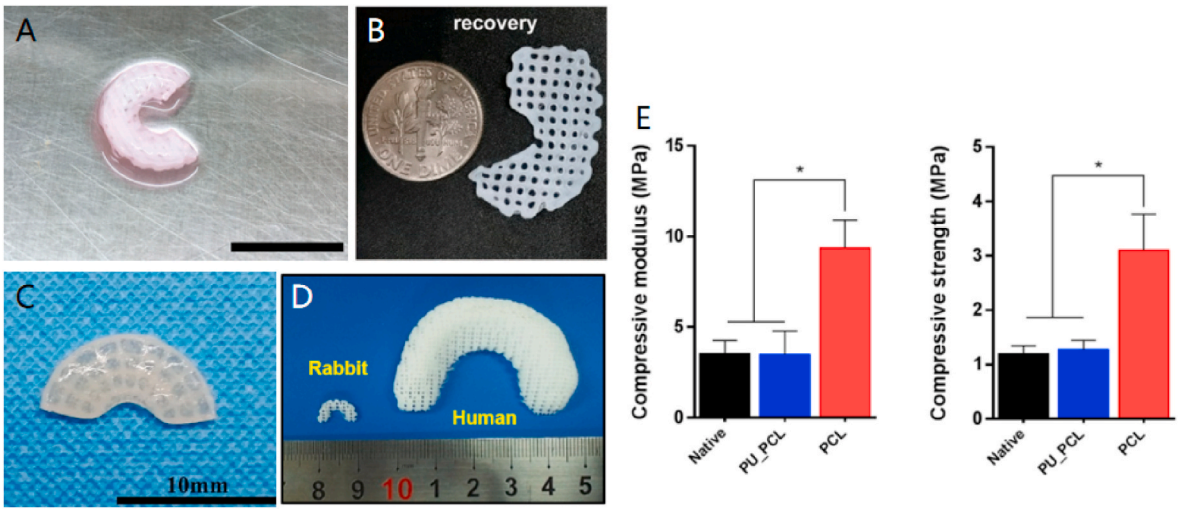

Fig. 5. Meniscus-mimicking constructs with different emphases. (A). 3D-printed PCL scaffold seeded with mesenchymal stem cells (scale bar represents 10 mm) [101]. (B). 3D-printed PVA/dECM scaffold [140]. (C). 3D-printed PCL scaffold infused with MECM-based hydrogel [27]. A muitilayer bionic meniscal scaffold was constructed by dual-nozzle printing (D) with oustanding mechanical properties (E) [147].

3.2. Stereolithography

Stereolithography refers to projecting a light source into photocurable bioink according to a predesigned program and realizing on-demand curing through the three-dimensional movement of the ink tank, thereby producing a customized structure [62]. At present, stereolithography appearance (SLA) and digital light processing (DLP) are commonly used in the field of tissue engineering [63]. In general, these techniques enable rapid preparation of target structures with high printing accuracy. However, it also has the disadvantages of high cost, difficulty integrating multiple materials and cells, and high dependency on photosensitive materials [64]. Therefore, the application of stereolithography in the field of cartilage-mimicking printing is considerably limited. Sarah et al. [65] utilized the DLP technique to print a simple architectural design consisting of a series of rigid columns filled with hydrogel and MSCs for cartilage repair (Fig. 4B). This study confirmed that scaffolds can effectively fill focal cartilage defects. However, there remains a demand for more systematic and comprehensive studies in this area.

3.3. Inkjet bioprinting

Inkjet bioprinting utilizes droplets as its fundamental unit of materials. These droplets can be as small as picoliters, and the printer has the capability of jetting thousands of ink drops per second, resulting in exceptional precision and high throughput. In addition, bioinks necessitate lower concentrations, as higher concentrations can cause the nozzles to clog [66], which is a completely different process compared to extrusion printing.

Due to the limitations of the fabrication principle, inkjet bioprinting is not ideal for constructing large-scale structures. Therefore, this method is frequently used in conjunction with other techniques for preparing cartilage-mimicking scaffolds. Tao et al. [67] first focused on electrospun polycaprolactone fibers to achieve optimal mechanical and organizational properties. Subsequently, biological properties were enhanced by supplementing the fibers with collagen hydrogels containing elastic rabbit chondrocytes through inkjet printing. After a week of cultivation, the cell survival rate exceeded 80 %. *In vitro* and *in vivo* experiments further confirmed that this design favored the deposition of type II collagen. Xavier et al. [68] employed a more sophisticated manufacturing technique that involved a combination of extrusion and inkjet printing (Fig. 4C). To replicate the collagen alignment of the meniscus, they started by creating anisotropic meniscus scaffolds with varying aspect ratios using melt electrowriting (MEW). Next, they utilized inkjet printing to inject cell-laden bioink into the PCL microchambers to enhance the biocompatibility of the scaffold, thereby completing the construction of a biomimetic multilayered meniscal scaffold.

3.4. 4D bioprinting

4D bioprinting is not a novel technology but rather builds upon 3D printing by introducing a time variable [69]. This technique allows structures created by 3D printing to be reshaped in response to external conditions such as temperature [70,71], pH [72], enzymes [73,74], magnetic fields [75], sound waves [76], light [77,78] and electricity [79,80], which will be fairly favorable for adapting to the dynamic environment in the human body. The emergence of 4D bioprinting offers more possibilities and promising prospects for the advancement of bionic bioprinting.

Recently, researchers have applied this technique to cartilage-mimicking printing. In particular, Pedro et al. [81] cleverly exploited the difference in swelling rates between tyramide-functionalized hyaluronic acid (HAT, high swelling) and alginate acid (AHAT, low swelling) to create a bilayer construct. This procedure allowed flexible adjustments to the morphology and curvature of the structure while maintaining high cellular activity. After 28 days of *in vitro* culture, the presence of new cartilaginous tissue was confirmed. Following a similar approach, Kim et al. [82] utilized the DLP technique to produce bilayer silk fibroin hydrogels and conducted finite element analysis to assess the shape changes of the intricate structures. The resulting hydrogels were then implanted into a tracheal defect model in rabbits, where the regeneration of both epithelial cells and chondrocytes was observed. In addition, there are some studies utilizing variations in photocrosslinking density to create intricate structures and verify the formation of 4D chondroid tissue [83].

4. Bionic materials

The level of biomimicry achieved in bioprinting is heavily influenced by the materials used in the construction of scaffolds. This relationship exists because the properties of the scaffolds are largely determined by the materials chosen. As such, the progress of bioprinting technology significantly relies on the development of material science. Due to the varying properties of different materials, researchers aim to consider a broader range of properties by expanding the selection of materials for

improved bionics and functional regeneration. Currently, typical materials used for cartilage-mimicking printing include natural materials, synthetic polymer materials, cells and cytokines.

4.1. Natural materials

Natural materials are biomaterials that are derived naturally, and their composition and structure closely resemble those of human tissue. This similarity makes them ideal materials for creating a microenvironment that can aid in tissue repair and is an excellent candidate for biomimetic printing. The commonly used biomaterials in cartilage tissue engineering include gelatin [84,85], hyaluronic acid [86,87], alginate [88,89], collagen [90], silk protein [91,92], acellular extracellular matrix [93,94] and others [95–97]. However, these materials usually have to undergo fixed processing, such as decellularization and enzymatic hydrolysis, to remove immunogenicity and acquire printability, resulting in the destruction of some of their molecular structures and loss of their original physical properties. Therefore, the lack of mechanical strength is a major problem for natural materials [98], especially when applied to cartilage tissue engineering. In addition, printability, shape fidelity, cell viability and biodegradation are also the focus of bionic printing.

Sang et al. [99] sought to create a bioink that could mimic the components of cartilage to a comprehensive degree. Their solution was a hybrid bioink composed of GelMA, HAMA, and chondroitin methacrylate sulfate (CSMA). To test the feasibility of the bioink, they conducted various analyses, including shape fidelity, swelling ratio, degradation, mechanical and rheological tests, and printability. The results demonstrated that the bioink maintained its original shape well, exhibited exceptional mechanical properties, and displayed satisfactory degradation behavior. They then proceeded to mix the ink with TGF-β1 and conducted some *in vivo* experiments. These experiments further confirmed that the biomimetic ink formulation is indeed advantageous for the regeneration of cartilage tissue.

4.2. Synthetic polymer materials

When compared to natural materials, polymers are characterized by a lack of biocompatibility, which can negatively impact their application in tissue engineering. However, they do offer good printability, adjustable degradation and controllable mechanical properties [100], making them indispensable choices for bionic bioprinting. As a result, polymer materials can be effectively utilized to optimize the morphological and mechanical simulation of the scaffold.

Zhang's research successfully leveraged these advantages. They printed a morphological bionic meniscal scaffold with PCL [101], optimized the mechanical properties of the scaffold by adjusting the pore size [102], and finally verified the effect of the scaffold through a series of animal experiments. The positioning of polymer materials has undergone a significant shift with the development of bionic concepts and printing technologies. Recent research studies [103–105] have increasingly utilized polymer materials as frameworks to enhance morphology and mechanics, while natural materials, cells, and cytokines have assumed critical roles in biological functions. These approaches have effectively bolstered the repair ability of scaffolds.

4.3. Cells

The limited number of cells in cartilage tissue and the scarcity of endogenous cells for recruitment pose a challenge for researchers seeking to improve repair outcomes. To address this issue, many studies have explored the potential benefits of adding a significant number of cells to the scaffold. Numerous studies have examined the value of various cell types in cartilage repair, including hyaline chondrocytes [106,107], fibrochondrocytes [108–110], elastic chondrocytes [111,112], and diverse mesenchymal stem cells [113–115].

Chondrocytes are a well-established source of seed cells due to their defined chondrogenic capacity and uniform composition. However, the source of autologous chondrocytes is restricted, and these cells are prone to aging and dedifferentiation during *in vitro* culture [116,117]. Therefore, it is difficult to obtain sufficient and high-quality chondrocytes from donors for cell expansion. MSCs are a type of adult stem cell that can be found in various tissues [118–122]. As *in vitro* targeted induction differentiation technology has matured, MSCs have become a popular research topic due to their advantages, including the ability to maintain their chondrogenic differentiation phenotype after large-scale expansion *in vitro*, easy sample collection, and reduced harm to donors. However, extensive research has revealed that the induction program is expensive and that the efficiency of induction is low. More importantly, early detection of gene expression related to chondrogenic hypertrophy, such as MMP13 and COL10, was found to result in significant vascularization and ossification *in vivo* after heterotopic transplantation [123]. Therefore, the selection of appropriate cells for biomimetic printing should be based on a given situation's specific needs. Furthermore, many studies varied widely [124,125] in their cell density designs, which may also be an important factor affecting the study validity.

4.4. Cytokines

The primary objective of incorporating cytokines into biomimetic printing is to replicate the endocrine and paracrine functions of the human body, enhance cell recruitment, and regulate cell behavior. Although not a mandatory element for biomimetic printing, cytokines do offer some beneficial effects on tissue repair. Currently, cytokines such as vascular endothelial growth factor (VEGF) [126], transforming growth factor (TGF-β) [127–129], fibroblast growth factor (FGF) [130], bone morphogenetic protein (BMP) [131,132], platelet-derived growth factor (PDGF) [133], and insulin growth factor (IGF-1) [134–136] are widely utilized. These cytokines will contribute to tissue repair by being incorporated into bioinks, added into microspheres, and chemically bound to biomaterials. However, in general, the use of cytokines in 3D printing is still in its infancy, and further research is required to fully understand their capabilities and mechanisms. More efforts are needed from researchers to fully explore the potential of cytokines in 3D printing.

5. Bionic progress of 3D bioprinted cartilage tissue

Human cartilage can be categorized into three types: hyaline cartilage (found in articular cartilage and the trachea), elastic cartilage (located in the auricle), and fibrocartilage (present in the intervertebral disc and meniscus). Each type of cartilage tissue possesses unique properties and functions, which must be accounted for when designing scaffolds. This section offers an overview of recent developments in bioprinting to mimic the various types of cartilage tissue.

5.1. Meniscus

The menisci are wedge-shaped fibrocartilage tissues located between the femoral condyles and the tibial plateau and are crucial for the movement of the knee joint. Regional differentiation is evident in the blood supply, cells, components, tissue structure and even innervation [137], resulting in a complex anisotropic structure that affects their morphology, function, and properties. Consequently, various bionic strategies have been developed for the meniscus Fig. 5, and the assessment of meniscal function recovery has multiple focuses Table 3.

Polymer materials are often a preferred choice for researchers due to their outstanding printability and mechanical properties. Additionally, their ability to achieve high printing resolution and shape fidelity makes them particularly suitable for constructing complex structures such as menisci. Zhang et al. [101] successfully printed a meniscus-like scaffold using PCL, which was then seeded with BMSCs and implanted into a

Table 3
Overview of the applications of bionic 3D bioprinting in meniscal regeneration.

Materials	Cell type	Biological cues	Characteristics	Results	Ref.
PCL	–	–	1. Morphological mimicry 2. The effect of PCL scaffold with different pore size	● *In vitro*, the scaffold with mean pore size of 215 μm optimized the cell behavior ● *In vivo*, it promoted the deposition of ECM	102.
PCL	BMSCs	–	1. Morphological mimicry 2. The effect of BMSCs	● BMSCs-laden PCL scaffold enhanced meniscal regeneration and mechanical strength	101.
PU, GG/HA/GA	–	–	1. Improvement of PU scaffold with composite materials	● The compression modulus, water absorption and contact angle were all improved ● After 7 days of culture *in vitro*, the expressions of type II collagen and GAG genes on the coated scaffolds increased	138.
GG/FB , SF-MA	MFCs	–	1. Morphological mimicry 2. Improvement of mechanical properties of the scaffold constructed with natural materials	● *In vitro*, the compressive modulus reached 353 kPa ● *In vivo*, the formation of regularly arranged collagen fibers was observed	139.
PVA/ECM	endothelial cells	–	1. Componential mimicry 2. The mix of synthetic and natural materials followed by specific processing techniques	● The hybrid ink had excellent mechanical properties and printability ● After 3 months *in vivo*, the scaffold could protect cartilage well and promote meniscal regeneration	140.
PCL, Alg/ECM	MFCs	–	1. Histological and componential mimicry 2. Preliminary attempt to take both histological and component into consideration	● The overall appearance and cartilage protection of the experimental group were good. ● The tissue structure, biochemical content and biomechanical properties were similar to those of the original meniscus	141.
PCL, ECM	–	–	1. Histological and componential mimicry	● The protection of articular cartilage and optimization of meniscus regeneration by the scaffold were demonstrated in rabbit and sheep experimental model	33.
PCL, AG, GelMA	MFCs	–	1. Morphological and histological mimicry 2. The immersion of different materials in the inner zone and outer zone to simulate anisotropic structure	● After 6 weeks of *in vitro* culture, cartilage-like tissue and fibrocartilage-like tissue could be seen inside and outside separately	32.
PCL, SF	SMSCs	L7	1. Morphological and mechanical mimicry 2. Focusing on retaining stem cells	● The histology, biochemical content, and biomechanical properties of the experimental group were very similar to those of a native meniscus	142.
PCL, GelMA/HAMA/ECM	–	KGN, PDGF-BB	1. Morphological and componential mimicry 2. The function of KGN/PDFG-BB and dual drug-releasing model	● The cytokines promoted cell migration, as well as direct cell differentiation to chondrogenic lineage, and markedly augmented meniscus regeneration	144.
PCL, 4-arm poly(ethylene glycol) amine-20 K, 4-arm poly(ethylene glycol) succinimidylester-20 K	BMSCs	Ac2-26, CTGF, TGF-β3	1. Morphological and histological mimicry 2. Anti-inflammatory and antioxidant microenvironment regulation and partitioned release of growth factors	● The scaffolds had good heterogeneous structure, biomechanical properties and anti-inflammatory and antioxidant effects ● Ac2-26 peptide was beneficial to zone-specific differentiation and expression of chondrocyte phenotypes	145.
PCL	BMSCs	CTGF, TGF-β3	1. Morphological and histological mimicry 2. The construction of the scaffold via triple-nozzle printing	● The cellular phenotype and matrix deposition of the regenerated menisci were similar to those of native menisci	146.
PCL, SF	–	–	1. Mechanical mimicry 2. Dual-nozzle printing	● The mechanical properties and biocompatibility were significantly improved	148
PCL/PU, ECM	BMSCs	–	1. Mechanical, morphological and componential mimicry 2. The mix of PCL and PU attained excellent mechanical properties	● The scaffold had a compressive modulus similar to that of the autogenous meniscus ● The new tissue also exhibited good mechanical properties in the rabbit model	147.
PCL, ECM/GelMA	MFCs	–	1. Morphological, componential and mechanical mimicry 2. Taking component, morphology, biomechanics, porosity, biodegradation. into account simultaneously	● A triple temperature control and dual-nozzle printing system for the printing of a multilevel bionic scaffold was developed ● The scaffold had outstanding shape mimicry, mechanical mimicry and compositional mimicry and the ability to promote meniscal tissue regeneration	60.

rabbit meniscus model that had undergone complete resection. After 24 weeks of observation, it was found that the meniscal scaffolds containing BMSCs were superior to the cell-free scaffolds, confirming that the scaffolds could improve the regenerative capacity and mechanical strength of the meniscus. Afterward, they [102] further studied the effects of PCL scaffolds with different pore sizes on cell function and tissue regeneration. The results suggested that the scaffolds with a pore size of 215 μm had better cell behavior and ECM deposition.

In their study, Farshad et al. [138] aimed to enhance the biocompatibility of polymeric materials by applying a coating of gellan gum (GG), HA, and glucosamine (GA) on polyurethane (PU) scaffolds. The findings indicated that the compression modulus, water absorption, and contact angle of the scaffolds were all enhanced. Moreover, after seven days of *in vitro* culture, the coated scaffolds exhibited increased expression of type II collagen and GAG genes.

Prior work has leveraged the excellent biocompatibility of hydrogels,

but their application in bionic bioprinting is hindered by mechanical properties and printing performance. In an effort to refine these properties, Costad et al. [139] mixed some natural materials to improve the mechanical properties. They used bioinks made of gellan gum/fibrinogen (GG/FB) and silk fibroin methacrylate (SF-MA) to fabricate highly elastic hybrid structures. After two weeks of *in vitro* cultivation, the compressive modulus reached 353 kPa. Following 10 weeks of subcutaneous implantation in mice, the formation of regularly arranged collagen fibers was observed. In contrast to this approach, some researchers [140] opted for a different strategy involving the mixing of poly(vinyl alcohol) (PVA) and ECM. This was followed by freezing/thawing cycles and alkaline treatment. Rheological and mechanical tests showed that the hybrid ink possessed excellent mechanical properties and printability. Subsequently, the incorporation of vascular endothelial cells into the bioink allowed for printing of the meniscal shape and implantation into a rabbit meniscus defect model. After a period of 3 months, it was observed that the scaffold was effective in protecting the cartilage and promoting meniscal regeneration.

The combination of printing and perfusion techniques is a practical and effective approach to integrating various materials. In a study by Chen et al. [141], a biomimetic meniscal scaffold was created by printing circular and radial PCL strands. This scaffold was then infused with an Alg/ECM composite hydrogel containing MFCs to enhance the bionic components and provide cells with an optimal microenvironment. Mechanical experiments demonstrated that the scaffold possesses compressive and tensile moduli comparable to those of the native meniscus. Following a 6-month implantation *in vivo*, the experimental group exhibited good overall appearance and cartilage protection, while the tissue structure, biochemical content, and biomechanical properties were similar to those of the original meniscus model. Li et al. [142] selected a combination of PCL and SF to achieve a balanced scaffold with desirable mechanical properties and degradation performance. The wedged frame was initially 3D printed using PCL and then filled with SF solution, which was subsequently crosslinked and lyophilized. To further enhance stem cell recruitment and retention, synovium-derived mesenchymal stem cell (SMSC)-specific affinity peptide (LTHPRWP; L7) was introduced. After 24 weeks of *in situ* implantation, the experimental group exhibited histology, biochemical content, and biomechanical properties similar to those of a native meniscus.

Li et al. [143] conducted a study on the effectiveness of another cytokine, kartogenin (KGN) in the regeneration of fibrocartilage. They began by preparing KGN-loaded microspheres using poly(lactic-*co*-glycolic acid) (PLGA), followed by 3D printing a PCL skeleton. They then injected the ECM gel, which contained the microspheres, into the pores to create a dual slow-release gel and microbead system. The chondrogenic ability of this system was ultimately confirmed through testing on a rabbit meniscus defect model. Following this, researchers [144] further refined their method by incorporating KGN-loaded PLGA microspheres and PDGF-BB into a GelMA/HAMA/ECM bioink and coprinted it with PCL. The results from *in vivo* experiments indicated that the scaffold was effective in promoting both cell migration and chondrogenic differentiation of MSCs.

In their study, Xu et al. [145] placed emphasis on regulating the microenvironment through anti-inflammatory and antioxidative means. To achieve this goal, they utilized a 3D printed porous anisotropic PCL meniscus scaffold, seeded it with BMSCs, and introduced the Ac2-26 molecule known for its anti-inflammatory and antioxidant properties. Additionally, they employed a rotation-immersion mold to add two growth factors (CTGF and TGF-β3) for spatiotemporal partition release. The outcomes of the study suggested that the Ac2-26 peptide had a positive impact on differentiation. Their findings revealed that the scaffolds possessed a heterogeneous structure with desirable biomechanical properties and anti-inflammatory and antioxidant effects. Moreover, the Ac2-26 peptide was observed to promote zone-specific differentiation, as well as the expression of chondrocyte phenotypes.

While the combination of printing and infusion can integrate a range of materials, the rough bionic level and complicated processing approaches present challenges for improvement. However, the introduction of multinozzle printing provides a convenient solution to this problem. In fact, Sun and colleagues [146] successfully constructed a scaffold using 3D printing alone, allowing the precise distribution of cytokines at fixed points. First, the physical support structure was created using fused PCL by extrusion printing. After, the hydrogel, which was loaded with BMSCs, was combined with microspheres of TGF or CTGF and printed into microchannels that were situated between the PCL fibers. This approach resulted in a faster and more convenient fabrication process. The 3D bioprinted meniscal scaffolds were then tested both *in vitro* and in a goat meniscal resection model. The findings indicated that the regenerated menisci displayed a similar cellular phenotype and matrix deposition to that of the native menisci.

Zhou et al. [60] dedicated to exploring multilevel bionics of meniscal constructs. Initially, they thoroughly examined the rheological properties of GelMA/ECM bioink before designing a personalized meniscal model that considered composition, appearance, and mechanics. Moreover, to print a multilevel bionic scaffold, they developed a customized triple temperature control and dual-nozzle printing system according to the features of the model and the bioink. Ultimately, through systematic *in vivo* and *in vitro* experiments, it was demonstrated that the scaffold exhibited exceptional characteristics such as mimicking the shape, mechanical properties, and composition of the meniscal tissue. Furthermore, it was also observed to effectively promote meniscal tissue regeneration.

Other researchers [147] utilized a similar technique to achieve better mechanical optimization. They adopted a PCL-PU blend as the framework and ECM for biocompatibility while using dual-nozzle printing as an engineered technique to create a biomimetic scaffold. The mechanical tests revealed that the scaffold had a compressive modulus comparable to that of the autogenous meniscus, and the new tissue also displayed favorable mechanical properties in the rabbit model.

5.2. Articular cartilage

Articular cartilage is a type of hyaline cartilage that covers the ends of joints. Its primary function is to act as a shock absorber and reduce friction between bones during joint movement. The histological structure of articular cartilage shows marked heterogeneity. For instance, the cartilage situated in the medial femoral condyle, a common site of osteoarthritis and sports injuries, is less than 3 mm thick, yet it comprises three distinct layers: the hyaline articular cartilage layer (2.41 mm), the calcified cartilage layer (0.13 mm), and the subchondral bone plate (0.19 mm). Regional differences in the distribution and arrangement of components and cells are evident in every layer [149,150]. However, due to limitations in the resolution and precision of current 3D printing techniques, fully bionic structures are difficult to achieve. As a result, researchers have focused on functional regeneration strategies for cartilage 3D bioprinting, which have gained increasing interest Fig. 6, Table 4.

Pores play a vital role in facilitating cellular substance exchange. However, in the case of cell-laden hydrogels, the nanoscale molecular network or the distance for substance exchange can often hinder cells from obtaining adequate nutrients. Li et al. [153] employed SF and gelatin (GT) to print macroporous hydrogel scaffolds at low temperatures, achieving a porosity of 70 %. They then seeded adipose-derived stem cells (ADSCs) using a combination of cell suspension and aggregation methods. This approach successfully regenerated cartilage structures and facilitated the integration of cartilage and osteochondral interfaces in a rabbit cartilage defect model. Chen and colleagues [154] utilized a comparable method, employing a low-temperature deposition technique to print ECM and water-based polyurethane (WPU), which

were subsequently lyophilized to create macroporous scaffolds. Following implantation into a rabbit cartilage defect model, the histological structure and mechanical properties of the repaired cartilage

Table 4
Overview of the applications of bionic 3D bioprinting in articular cartilage regeneration.

Materials	Cell type	Biological cues	Characteristics	Results	Ref.
SF, GT	ADSCs	–	1. The exploration of porous structure and cell aggregate	● The porosity of the scaffolds reached 70 % ● The satisfactory regenerated cartilage structures, integration of cartilage and osteochondral interfaces *in vivo*	153.
ECM, WPU	ASDCs	–	1. Hierarchical macro-microporous structure	● The histological structure and mechanical properties of the repaired cartilage resembled those of normal tissue	154.
SF, GT	BMSCs	E7	1. The introduction of E7	● The addition of E7 made the new cartilage more closely resemble the autogenous tissue from HE, MRI, SEM	155.
b-TPUe, colI/PBA	–	–	1. Mechanical mimicry	● The mechanical property of b-TPUe scaffold was considerably close to native cartilage ● A greater cell count and increased ECM deposition	156.
PLA, HA	ACCs	–	1. Investigation of compressibility, degradation and biocompatibility of HA	● PLA/HA scaffolds favored the expression of chondrogenic gene markers and specific matrix deposition	157.
GelMA, PCL-hydroxyapatite	–	IL-4	1. Histological mimicry 2. The introduction of IL-4	● The histological score of bilayer scaffolds containing IL-4 was twice that of ordinary scaffolds	158.
GelMA, HA	–	–	1. Histological mimicry 2. The value of interfilamentous spacing	● *In vivo* experiments showed that the scaffold promoted cartilage regeneration well ● The interfilamentous spacing played an important role in cell migration and nutrient osmosis	159.
Alg, GelMA, CS, TCP	BMSCs, ACCs		1. High-level gradient histological mimicry 2. The introduction of microfluidic print	● Constructs with gradient differences were conducive to cartilage regeneration and the maintenance of cartilage phenotype	160.
PCL, HA	–	TGF-β1, BMP-7, and IGF-1	1. Histological mimicry 2. The construction of gradient structure 3. The introduction of MEW	● Differences among the layers led to regional heterogeneity of chondrocytes and ECM, promoting functional regeneration	161.
PLCL, aggrecan	–	–	1. Aggrecan combined with the PLCL scaffolds by covalent bond	● *In vivo*, functionalized scaffold treated with aggrecan doubled the thickness of the regenerated cartilage tissue ● The number of chondrocytes and type II collagen increased significantly	165

were similar to those of normal tissue after six months.

In their study, Shi et al. [155] mainly aimed to address the issue of natural materials with insufficient mechanical properties. They developed a bioink with appropriate mechanical properties and degradation speed for cartilage regeneration by adjusting the ratio of SF and GT. To further enhance cell recruitment, a BMSC-specific affinity peptide was incorporated into the scaffold and BMSCs were seeded within it. Finally, the effectiveness of the bioink was confirmed in a rabbit microfracture cartilage defect model. Daniel et al. [156] took a different path to print thermoplastic polyurethane 1,4-butanediol (b-TPUe) that exhibited mechanical properties similar to those of cartilage. To improve cell adhesion, they coated collagen type I and 1-pyrenebutyric acid (PBA) onto the b-TPUe scaffolds, taking into account both the material's mechanical properties and biocompatibility. Cristina et al. [157] conducted a study on the compressibility, degradation properties, and biocompatibility of HA. They then injected HA hydrogel, which contained articular chondrocytes (ACCs), into the pores of polylactic acid (PLA) scaffolds and cultured them *in vitro* for one month. The results showed that PLA/HA scaffolds were more effective than simple PLA scaffolds in promoting the expression of chondrogenic gene markers and specific matrix deposition.

In addition, some researchers focused on the histological structure of the cartilage layers and performed biomimetic printing. Lin and colleagues [158] developed a bilayer scaffold and explored the potential of interleukin-4 (IL-4) for cartilage regeneration. They used digital light processing (DLP) to print GelMA mixed with IL-4 on the upper layer, while fused deposition modeling (FDM) was employed to create porous PCL and hydroxyapatite on the lower layer. The results of *in vivo* experiments demonstrated that the histological score of the bilayer scaffolds containing IL-4 was twice as high as that of the ordinary scaffolds. Gao et al. [159] utilized continuous printing of GT and GelMA-HA to create a double-layered porous scaffold. The researchers also investigated the impact of interfilamentous spacing on scaffold performance. After observing the scaffold's effectiveness in promoting cartilage regeneration over a 12-week period in a rabbit tracheal defect model, they discovered that interfilamentous spacing played an important role in cell migration and nutrient osmosis, but various materials and models required different parameters for interfilamentous spacing.

Microfluidic printing is a promising method for achieving high shape fidelity and preserving cell viability. In a study by Joanna et al. [160], this technique was utilized to create inks (Alg, GelMA, chondroitin sulfate (CS), HAMA, β-tricalcium phosphate (TCP)) with varying concentrations and cell types (BMSCs and ACCs), resulting in bionic cartilage and osteochondral layers with gradient structures that demonstrated excellent shape fidelity and cell viability. Through *in vitro* culture and testing on rabbits, it was confirmed that these gradient differences were conducive to cartilage regeneration and the maintenance of the cartilage phenotype.

Yu et al. [161] utilized the MEW technique, which offers higher printing resolution than FDM, and combined it with inkjet printing to deposit various cytokines at different layers. Specifically, TGF-β1 and BMP-7 were deposited on the surface layer, IGF-1 on the middle layer, and HA on the deep layer. This approach allowed for more accurate structures with histological bionics. As a result, the composite scaffold was able to effectively improve cell behavior. Additionally, the differences among the layers led to regional heterogeneity of chondrocytes and ECM, which promoted functional regeneration.

Shim et al. [162] focused more on the potential toxicity and inconvenience of cross-linking agents. Consequently, they opted for a material that does not require cross-linking, specifically cucurbit [6]uril (CB [6]) and polyamine (PA). These two molecules are able to interact with each other in the presence of stem cells, forming noncovalent bonds. To synthesize CB [6]-HA and DAH-HA, the researchers modified HA with these two molecules. Next, they coprinted these inks with pepsin-treated collagen (atelocollagen), PCL, and turbinate-derived mesenchymal stromal cells (TMSCs) to create a multilayer structure. After 8 weeks of implantation in a rabbit model, it was found that layered collagen and HA yielded greater benefits for the regeneration of osteochondral tissue than Alg.

The osteochondral defect, being a severe joint injury, serves as a crucial risk factor for the progression of osteoarthritis and thus has been the primary focus of research on articular cartilage therapies [163]. When it comes to 3D bioprinting, constructing osteochondral scaffold often encounters multiple challenges such as histological disparities,

interface stability, and an increase in uncertain variables. These factors significantly amplify the complexity of conducting research in this field. Liu et al. [110] developed multilayer scaffolds incorporating BMSCs and diclofenac sodium (DC) to address the common challenges of endogenous chondrocyte deficiency and inflammatory response in osteochondral defect repair. The subchondral bone layer was composed of PCL, while the cartilage layer consisted of KGN-loaded PCL and BMSCs-laden methacrylated hyaluronic acid (MeHA) hydrogel. Additionally, a matrix metalloproteinase (MMP)-sensitive drug delivery hydrogel coated with DC applied on top of the scaffold. Results demonstrated that the scaffold effectively enhanced cartilage regeneration by promoting type II collagen deposition and suppressing interleukin 1β secretion. Furthermore, in an animal model, the scaffold improved joint function in terms of ground support force, paw grip force, and walking gait parameters. Focusing on the clinical translational potential, Li et al. [164] developed a cell-free exosome-loaded bionic ECM double-layer scaffold. This scaffold constructed a dual network by crosslinked GelMA and Schiff's base bond, enabling controlled and continuous release of exosomes. *In vitro* experiments validated the scaffold's ability to enhance cellular behavior and facilitate osteogenic differentiation. Subsequently, the authors implanted this scaffold in a preclinical model, where histological staining and imaging demonstrated its capacity to promote regeneration of both cartilage and subchondral bone, potentially attributed to the sustained release of MSC-derived exosomes. The authors propose that this strategy holds promise as a solution for clinical cartilage injury.

5.3. Auricle

The auricle, which is the external part of the ear, is composed of elastic cartilage tissue covered by a layer of skin. Elastin is the primary component of auricular cartilage, providing it with exceptional flexibility. Additionally, the complex shape of the auricle is necessary for collecting sounds. Consequently, bionic bioprinting of the auricle focuses on replicating its appearance and elasticity Table 5.

Some studies initially focused on the shape of the auricle. In a study by Bok [166], the details of auricular modeling were explored and a high-level shape-mimicking auricular scaffold was printed using PCL. However, functional verification was not carried out. Liu et al. [167] used a bioink blended with albumen/alginate/gelatin (A-Alg-GT) and HUVECs to print a shape-mimicking scaffold, which was verified to exhibit biocompatibility and vascular support behavior *in vitro*. Similar studies were conducted by other researchers using different materials and cells [168–171].

Dafydd et al. [172] focused on improving biomimetic composition and conducted a thorough investigation of the ECM. They synthesized a practical material called ECMMA, which could be utilized for photocrosslinking. Additionally, he took advantage of proteomics techniques to analyze the differences between ECM and native tissue. While there were some compositional discrepancies between the two, the ECM still retained many functional components and demonstrated superior biomimetic composition when compared to other materials. Then, they printed the auricular scaffolds and cultivated them for 28 days. It was found that the cartilage components in the ECMMA group were significantly greater than those in the GelMA group.

Table 5
Overview of the applications of bionic 3D bioprinting in auricle regeneration.

Materials	Cell type	Biological cues	Characteristics	Results	Ref.
PCL	–	–	1. Morphological mimicry 2. The exploration of printing model	● Achieving the high-level morphological imitation of auricle	166.
GelMA, nanoclay	–	–	1. Morphological mimicry 2. The function of nanoclay	● The addition of nanoclay in GelMA improved the porosity, mechanical strength and the degradation ratio	168.
ECM, PVA, Gel	–	–	1. Morphological and componential mimicry	● *In vivo* results revealed the regeneration of cartilage specific matrix, including collagen and elastin	169.
cellulose microfiber	–	–	1. Morphological mimicry 2. High-resolution printing with natural materials	● The resolution of auricular scaffold reached 250 μm with cellulose microfiber by DIW	170.
SF, GT	ECCs	–	1. Morphological mimicry 2. No crosslinking	● The SF-Gel hydrogel optimized shape fidelity, swelling capability, degradability, and compressive strength ● The increased expression of SOX9, ACAN, ColII was observed in bioprinted constructs	171.
ECMMA	ECCs	–	1. Morphological and componential mimicry	● Compared with GelMA group, the ECMMA group achieved more cartilage ECM components	172.
GelMA	ECCs , ADSCs	–	1. Morphological mimicry 2. Noninvasive bioprinting by near infrared (NIR) photopolymerization (DNP)	● After subcutaneous implantation in mice for 1 month, the scaffold could maintain its shape and promote the expression of type II collagen in cartilage lacuna	173.
PCL, HA, Alg	–	–	1. Morphological and mechanical mimicry 2. Dissolving PCL in organic solvent to improve the mechanical strength and simplify the procedure	● The heterogeneous localized surface tension was similar to the natural ECM	174.
PLA, GelMA	ECCs	–	1. Morphological and mechanical mimicry 2. The combination of synthetic materials and natural materials.	● *In vitro*, the experimental group exhibited good proliferative properties and cellular activity ● *In vivo*, new chondrocytes and chondrogenic matrix could be observed	175.
GT, FB, HA, Gly	ECCs	–	1. Morphological and mechanical mimicry 2. Advanced and comprehensive design of the model	● *In vitro*, the histological components resembled the human ear ● *In vivo*, the similar elastic character was observed as native tissue in 4 weeks	176.
ECMMA, GelMA, PEO, PCL	ECCs	–	1. Morphological, componential and mechanical mimicry 2. High-level mimicry at different perspectives	● Using dual-nozzle printing to integrate different materials to achieve precise shapes, low immunogenicity, and excellent mechanical strength ● *In vivo*, the high morphological fidelity, excellent elasticity, abundant cartilage lacunae, and cartilage-specific ECM deposition were attained	177.
A-SA-Gel	HUVECs	–	1. Morphological mimicry 2. The study of vascular support behavior	● A-SA-Gel hydrogel scaffold had good cell compatibility and vascular supportive behavior	167.
PCL, Alg, PEG	ADSCs, CCs	–	1. Morphological mimicry 2. The attempt of multinozzle printing for auricle	● Successful application of sacrifice materials and separate printing of different cells	178

In their research, Chen et al. [173] implemented a highly sophisticated printing method that significantly streamlined the entire process. Their approach utilized digital near-infrared (NIR) photopolymerization (DNP) 3D printing technology to create auricular scaffolds that were noninvasively printed under the skin of nude mice and then cultured for a month. The outcome of the experiment was that the scaffold retained its original shape, and there was a significant secretion of type II collagen observed in the lacunae of cartilage.

Lei et al. [174] employed a unique method to enhance the mechanical properties of their scaffold. To create the scaffold, PCL particles were initially dissolved in a precursor solvent consisting of mixed dichloromethane (DCM) and dibutyl phthalate (DBP). This solution was then used to uniformly encapsulate both the PCL liquid and hydroxyapatite nanobioceramics. After adjusting the ratio, Alg was added to complete the scaffold printing process, which was then cross-linked using calcium chloride. These researchers also used this bioink to produce a gyroid scaffold via direct ink writing (DIW) and confirmed that its uneven local surface tension was comparable to that of natural ECM. In summary, this study combined the mechanical properties and biocompatibility of two materials, eliminating the need for sacrificial materials or high-temperature melt deposition and simplifying the printing process and requirements. In contrast, Tang et al. [175] used a more conventional approach of printing and perfusion to achieve their desired effect.

A multinozzle printing system has also been utilized in 3D bioprinting of the auricle. Hyun-Wook et al. [176] developed an integrated tissue-organ printer (ITOP) that used GT/FB/HA/glycerol and rabbit ear chondrocytes (ECCs) with a cell density of 40 $\times$ 10^6 cells/ml as the bioink. PCL was used as the framework to create the bionic pinna scaffold. The scaffold was also designed to ensure sufficient pore preservation, allowing for the exchange of oxygen and nutrients. Histological staining revealed that the new tissue composition and structure closely resembled that of the human ear. Additionally, *in vivo* experiments demonstrated comparable elasticity to that of the rabbit ear. These promising findings are likely due to the meticulous design of the printed model and the abundance of chondrocytes present.

Jia et al. [177] further improved the design of the scaffold by accounting for factors such as shape, elasticity, and microenvironment. They combined the benefits of ECMMA, GelMA, poly(ethylene oxide) (PEO) and PCL to attain a precise appearance, low immunogenicity, and excellent mechanical properties. After 24 weeks of subcutaneous implantation in nude mice, the experimental group showed noticeable morphological fidelity, excellent elasticity, plentiful cartilage lacunae, and cartilage-specific ECM deposition.

5.4. Trachea

While the trachea's anatomy is fairly complex, it can be simplified into three layers: the mucosal, submucosal, and adventitial layers. The adventitia, which is the central component, is supported by 16–20 C-shaped hyaline cartilage rings that are connected by membranous ligaments made of elastic fibers. These cartilage rings have a notch that faces the trachea's posterior wall, and there are ligaments and smooth muscle bundles in the gap between them [179,180]. The mucosal layer serves as a crucial barrier for the trachea. Without it, granulation tissue may proliferate in the lumen, which could ultimately lead to death [181]. The submucosa is composed of loose connective tissue that contains numerous glands. As a result, constructing a bionic tracheal scaffold involves several factors that can influence its success, and evaluating functional recovery cannot be based solely on the formation of cartilaginous tissue Table 6.

Gao et al. [182] created a tracheal scaffold using poly(L-lactic acid) (PLLA) with biomimetic morphology. Autologous ECCs were then seeded onto the scaffold. After two weeks of *in vitro* culture and two weeks of *in vivo* paratracheal muscle culture, the engineered tracheal and pedicled muscle flaps were transplanted into a tracheectomy rabbit

Table 6
Overview of the applications of bionic 3D bioprinting in trachea regeneration.

Materials	Cell type	Biological cues	Characteristics	Results	Ref.
PLLA	ECCs	–	1. Morphological mimicry	● Epithelization could be successfully achieved and overgrowth of granulation tissue seldom occurred in experimental group	182.
PCL, PLA/GT	–	–	1. Morphological and mechanical mimicry 2. The combination of different TE techniques	● The compressive modulus was close to that of natural tissue ● Cartilage-like tissue gradually formed in mice for 8 weeks	183.
SF, GMA	FCs, NCCs	–	1. Morphological mimicry	● The ink was conducive for the proliferation and differentiation of chondrocytes *in vitro* ● New cartilaginous tissue and cells appeared near the transplanted scaffold	184.
SFMA	ECCs	–	1. Morphological and mechanical mimicry 2. The application of 4D bioprinting	● Rapidly photocrosslinked silk-MA bioink could flexibly regulate biodegradation, mechanical strength and printability ● Bronchoscopy revealed entire recovery of lumen and mucosa and relatively immature neocartilage tissue	185.
PCL, atelocollagen	NCCs, NTSCs	–	1. Morphological and histological mimicry 2. Delicate design for the histological structure of tracheal scaffold	● *In vivo*, many infiltrating microvessels could be seen around the regenerated cartilage ● Histological staining revealed the formation of mature chondrocytes and cartilage-like ECM	43.
PCL, silicon, Collgen, ECM	NTSCs	–	1. Morphological and histological mimicry 2. Multilayer and detailed simulation for trachea	● After 2 months *in vivo*, histological staining showed the formation of trachea-like tissue ● The expression of cell-specific markers in basement membrane and angiogenesis were observed in specific stainning	186.
GelMA, ECMMA, DMMA, CSMA, HAMA	ECCs, HUVECs, fibroblasts	8-arm-polyethylene glycol-succinic acid ester (8-PEG-NHS)	1. Morphological, componential and mechanical mimicry 2. Adequate componential and cellular design for discrepant structure	● X-ray and tracheoscopy showed that the trachea returned to a good recanalization, seamless connection of the defect site of the primary trachea and complete epithelial regeneration	187.
Alg, ECM	–	–	1. Morphological and componential mimicry 2. Printing in suspended hydrogel	● Mature epithelial cell types in airway lumens were observed *in vitro*	188

model. Their histological results showed successful epithelization in the experimental group, with minimal overgrowth of granulation tissue.

Nilesh et al. [183] utilized a combination of 3D printing and electrospinning to create a porous PCL scaffold. Subsequently, a short nanofiber dispersion of polylactic acid/gelatin (0.5–1.5 wt%) was electrospun onto the scaffold surface, after which ECCs were added. Mechanical property tests indicated that the compressive modulus of the scaffold was similar to that of natural tissue. When the scaffold was implanted subcutaneously in mice for 8 weeks, cartilage-like tissue gradually formed.

Gao et al. [184] more closely considered the cytocompatibility of materials and developed a bioink called SF-glycidyl-methacrylate (GMA) that is suitable for DLP 3D printing. *In vitro* experiments demonstrated that ink promotes the proliferation and differentiation of chondrocytes. Subsequently, the printed scaffold was implanted into a rabbit tracheal defect model, resulting in the appearance of new cartilaginous tissue and cells near the transplanted scaffold.

Jung-Seob et al. [185] utilized similar materials and further expanded their applications. Initially, the researchers prepared a silk-MA bioink that could be rapidly photocrosslinked, allowing for the regulation of biodegradation speed, mechanical strength, and printability. Using DLP, they printed various tissue structures, such as the trachea, and performed preliminary experiments to confirm their chondrogenic ability. Furthermore, the material possessed the unique ability to change shape even under physiological conditions. As a result, the researchers utilized it for 4D printing of the trachea, which was then implanted into a partial defect model. Following a period of 8 weeks in culture, bronchoscopy revealed complete restoration of the lumen and mucosa, along with relatively immature neocartilage tissue.

The design developed by Hu et al. [186] represents a significant advancement in tracheal mimicry, elevating it to a new level of sophistication. They incorporated a trachea-mimicking bellows scaffold that was printed indirectly with PCL. To reinforce the structure, silicone rings were added. The luminal surface was then coated with collagen and ECM hydrogels in sequence. Finally, TMSC sheets were added to achieve a multilayer simulation of the histological structure. This complex design was truly remarkable in its attention to detail and dedication to mimicking natural structures. After being cultured *in vivo* for 2 months, histological staining revealed the development of trachea-like tissue and the expression of cell-specific markers in the basement membrane and angiogenesis, as observed through specific staining techniques. In general, this study did not rely heavily on 3D printing elements, and the preparation process was somewhat complex.

It is widely recognized that cartilage relies on the surrounding tissue for proper nutrition. Consequently, to further achieve better functional regeneration, Huo et al. [187] exploited a 3D printing strategy to obtain a cartilage-vascularized fibrous tissue-integrated trachea (CVFIT). First, to better simulate tracheal cartilage and surrounding tissue, the researchers prepared various materials separately, including ECMMA, GelMA, CSMA, ADMMA, HAMA, and 8-arm succinic acid ester (8-PEG-NHS). These materials were combined in specific ratios to mimic the components of the primary trachea and connective tissue. The goal was to achieve satisfactory results in terms of both mechanical properties and appearance. Afterward, the scaffold was preimplanted and wrapped by a vascular muscle flap in a rabbit neck for 8 weeks and then implanted in a tracheal defect model *in situ*. X-ray and tracheoscopy showed that the trachea returned to good recanalization, seamless connection of the defect site of the primary trachea and complete epithelial regeneration, indicating that the function of the trachea had been well restored.

5.5. Other cartilage tissue

Certain cartilage tissues have received relatively scarce attention in previous studies, which is generally attributed to limited knowledge or few dedicated research effort. Here, we provide a concise summary of the prior studies

The nose is a vital aesthetic organ, with breathing and olfaction being its crucial functions [189]. Therefore, nasal damage or deformity can significantly impact patients' physical and mental well-being. Currently, autologous cartilage transplantation and artificial implant treatment are commonly used methods; however, they often fail to yield satisfactory results for reasons such as infection, secondary surgical injury, donor scarcity, and high resorption rates [190,191]. The utilization of 3D printing enables precise fabrication of customized models, thereby offering a partial solution to the aforementioned issues, rendering it highly favored among researchers.

The advantages of 3D printing were fully explored by Hee-Gyeong et al. [192] to prepare personalized customized models. In this study, the shapes of preoperative and virtual postoperative noses were analyzed, and the octahedral interior architecture was designed using CAD software. Subsequently, a cartilage-derived hydrogel mixed with ADSCs was injected into the nasal implant. *In vitro* experiments confirmed the scaffold's potential to induce cartilage differentiation of ADSCs. Additionally, significant chondroid tissue deposition was observed after subcutaneous implantation of mice, supporting that the scaffold effectively combined the advantages of autologous cartilage and artificial nasal scaffold.

Lan et al. [193] conducted further systematic verification of the *in vivo* and *in vitro* cartilage formation ability of 3D bioprinted scaffolds. Considering the requirements for surgical suturing and skin shrinkage during clinical application, the researchers investigated the influence of culture time on the mechanical properties and ECM formation ability of a 3D bioprinted Type I collagen hydrogel scaffold containing chondrocytes. Initially, they successfully prepared the scaffold using the freeform reversible embedding of suspended hydrogels (FRESH) bioprinting method (Fig. 7A) and confirmed its high cellular activity (>85 %). To compare with clinically approved type I/III collagen membrane scaffolds (Chondro-Gide), which served as the control group, immunofluorescence tests were performed after a certain period of *in vitro* culture. The results indicated that both groups secreted a significant amount of type II collagen, but the secretions were more uniformly distributed in the bioprinted group (Fig. 7B). The quantitative analysis of gene expression revealed no significant difference between the two groups (Fig. 7C). The researchers subsequently conducted a more comprehensive comparison of *in vitro* and *in vivo* grown implants, which included Safranin-O staining, Masson's Trichrome staining, and immunofluorescence for type I and II collagen (Fig. 7D). The results demonstrated that both the bioprinted group and the control group exhibited a lack of peripheral proteoglycan deposition, whereas this issue was not observed in the parallel group *in vitro*. However, both *in vivo* and *in vitro* experiments showed that the bioprinted group produced higher levels of collagen than the control group, approaching those found in autologous tissue. Finally, mechanical properties were assessed for both groups revealing no significant difference in bending modulus; furthermore, noticeable improvements were observed after implantation.

As a crucial load-bearing joint structure, intervertebral discs (IVDs) enable flexion, extension, and rotation in the spine. These functions rely on its intricate organizational structure, encompassing the outer annulus fibrosus and inner nucleus pulposus, as well as the anterior and posterior longitudinal ligaments and superior and inferior end plates [194]. IVD dysfunction is among the most prevalent clinical diseases. While conservative treatment falls short of providing a comprehensive solution, surgical intervention may adversely impact the spinal range of motion or adjacent vertebral degeneration [195]. Tissue-engineered scaffolds from 3D bioprinting present a promising approach for their management.

Damage to the annulus fibrosus is a significant contributor to IVD degeneration. Therefore, Liu et al. [196] were dedicated to simulating the microstructure and mechanical properties of annulus fibrosus. By employing a newly developed electrohydrodynamic 3D printing technique, an angle-ply architecture was fabricated to enhance printing resolution and simulate the arrangement of fiber rings. As a result, the

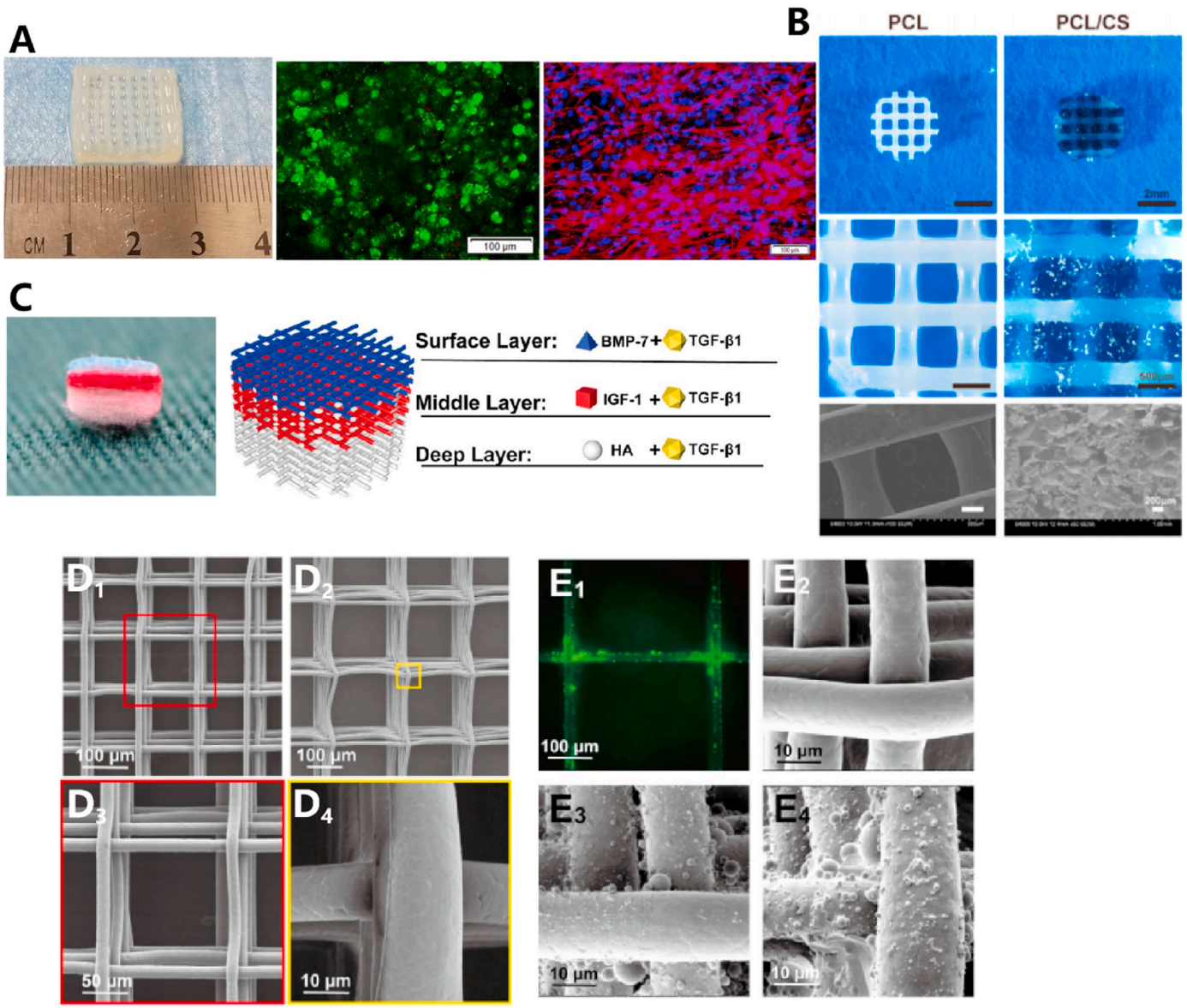

Fig. 6. Development of cartilage-mimicking constructs. (A). Single-material scaffold: 3D bioprinted cell-laden alginate/collagen scaffold (Left) with a focus on cell viability (Middle, Calcein-AM/PI staining) and cytocompatibility (Right, Rhodamine–phalloidin/Hoechst 33,258 staining) [151]. (B). The design of the hybrid scaffold was achieved by the combination of the support of the PCL frame and the cytocompatibility of chitosan (CS) hydrogel [152]. C-E. Composite biophysic scaffold with osteochondral bionics constructed by a multihead printing system. Fine bionics for multilayered cartilage tissue with delicate selections of cytokines (C) [161]. Precise MEW printing with extremely high resolution (D). Image of green (FITC) fluorescent microspheres adhering to the scaffold (E1) and comparison of SEM images of a simple scaffold (E2), microsphere-attached scaffold (E3) and microsphere-adherent scaffold (E4).

'x' type scaffold demonstrated higher tensile stress (2.8 ± 0.4 MPa), ultimate strain (65.8 % ± 6.2 %), and ultimate strength (6.9 ± 0.4 N) compared to the '+' scaffolds; however, there was still some disparity with human disc performance [195]. Subsequently, the researchers combined the scaffold with GelMA hydrogel that mimics the nucleus pulposus in order to construct tissue-engineered intervertebral discs (TE-IVDs). These TE-IVDs were then implanted into a rat model for total disc replacement, where they observed maintenance of disc height, reduction in loss of NP water content, and partial restoration of IVD biomechanical function.

Sun et al. [197] focused on studying the repair effect of bionic scaffolds by dual-factor strategy. They loaded connective tissue growth factor (CTGF) and TGF-β3 onto polydopamine nanoparticles and mixed them with gelatin/sodium alginate/HA hydrogel. The resulting mixture was then coprinted with PCL to fabricate the structure of the bionic annulus fibrosus and nucleus pulposus. *In vitro* experiments confirmed that the two factors could be released in a spatially controlled manner, allowing BMSCs to differentiate into nucleus pulposus-like and annulus fibrosus-like cells. Subcutaneous transplantation experiments in nude mice demonstrated that the scaffold exhibited a zone-specific matrix, with the core area mainly composed of type II collagen and glycosaminoglycans and the surrounding area mainly composed of type I collagen.

6. Conclusions and future prospects

In conclusion, 3D bioprinting is the most effective technology for manufacturing and distributing materials, cytokines, and cells. The concept of bionics is also the most important basis that has inspired innovation and guided research design in 3D bioprinting [198]. Over years of development, experts in diverse fields have communicated and collaborated, leading to remarkable achievements in bionic 3D bioprinting as an interdisciplinary subject within the medical field. The

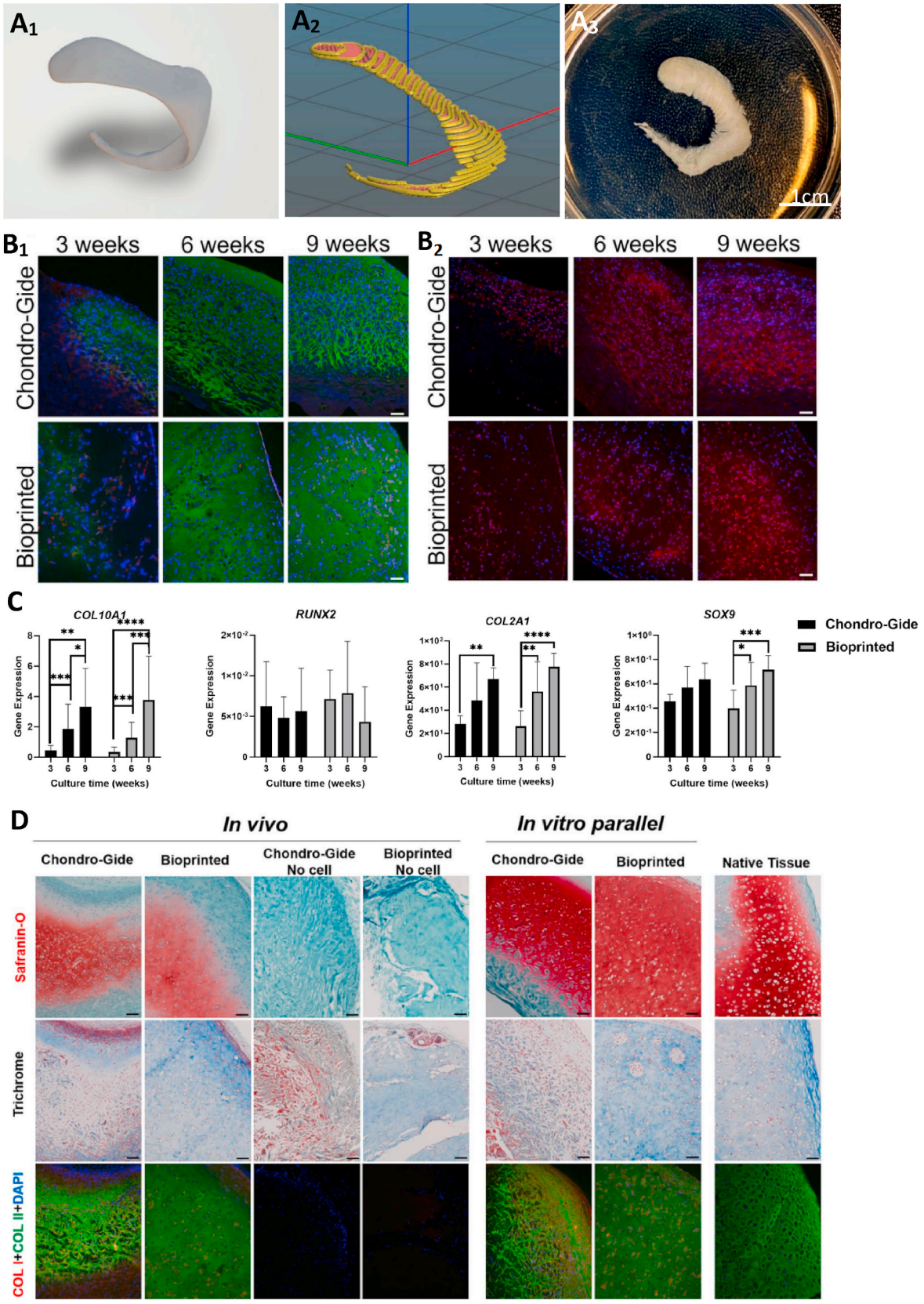

Fig. 7. *In vitro* and *in vivo* cultivation of bioprinted human nasal cartilage [193]. (A_1) 3D model of a right lower lateral nasal cartilage from CT imaging and (A_2) the preview of the sliced nasal cartilage. (A_3) 3D bioprinted lower lateral nasal cartilage. (B). Immunofluorescence of *in vitro* constructs across culture time. (B_1) Type I (red) and II (green) collagen and (B_2) type X collagen (red). The blue color is from DAPI staining (scale bar = 100 μm). (C). Gene expression of *in vitro* constructs. (D). Histology and immunofluorescence of chondrogenic related proteins (scale bar = 100 μm).

combination, modification and mixing of different materials, the exploration and selection of a variety of cells, the addition of specific cytokines and the impressive design concepts together promote the progress of bionic 3D printing. However, reviewing existing studies reveals that most prior research is limited to achieving a specific histological structure and functional recovery and falls short of the comprehensive restoration of native tissue. While several studies have attempted multidimensional mimicries, there is currently no established standard for the level of biomimetics, and further rigorous evaluation is needed to determine its value. For instance, the bionic structure of circular and radial material arrangement as a representation of meniscal tissue structure raises questions, and its significance in tissue repair requires more scientific evidence due to the nanometer-scale resolution of meniscal collagen arrangement compared to the typical resolution of many 3D printing techniques which exceeds 100 μm. Moreover, it is inaccurate to conclude that cartilage tissue production solely relies on collagen and GAG synthesis since the functionality also depends on complex types of collagen and regular fiber alignment.

In fact, one of the most significant goals of 3D bionic bioprinting is to construct organoids, but the drawbacks of this technique clearly limit the design of complex macrostructures and fine microstructures, which is attributed to a fundamental discrepancy between the rapid layer-by-layer process of 3D bioprinting and the long-term growth and development of organs. As a result, researchers often need to cultivate original constructs *in vitro* or *in vivo* for an extended period before conducting animal experiments. The author believes that research in the field of 3D bioprinting should focus not only on the characteristics of the tissue but also on the growth process of tissue and organs. Cells may play the most critical role in this process. Additionally, with 3D bioprinting having reached an advanced phase, and the integration of multiple tissue-engineered techniques and unique designs could soon make significant contributions to effective progress in bionic manufacturing techniques.

The ultimate objective of biomimetic bioprinting is the treatment of diseases. Currently, traditional 3D printing without living cells and bioactive materials has been utilized by certain researchers in some fields such as anatomical visualization for educational purposes or preoperative planning [199], as well as prosthetic implantation [200]. However, the clinical translation of bioprinted structures tend to require a series of *in vitro*, *in vivo* and clinical trials. Although certain studies have demonstrated promising outcomes in both *in vivo* and *in vitro* experiments, suggesting their potential for clinical translation, it should be acknowledged that clinical diseases often exhibit diversity and dynamics, which necessitates strict experimental conditions. Moreover, addressing intricate ethical and biosafety concerns are also imperative for successful clinical translation. Therefore, a significant challenge facing 3D bioprinting lies in determining how to achieve improved solutions for these issues. The effective development of animal experiments is a prerequisite for clinical trials. Currently, most studies on 3D bioprinted cartilage-mimicking constructs are conducted *in vivo* using small animal models, such as subcutaneous transplantation in nude mice and disease models in rats or rabbits. However, it should be noted that the anatomical structure and mechanical environment of these animals differ significantly from those of humans, necessitating further validation of their relevance to clinical research. In contrast, certain large animals like monkeys and sheep may exhibit greater similarity to the mechanical environment found in humans. Therefore, there is an urgent need for the development of large animal disease models and corresponding animal experiments.

The clinical trial research on tissue-engineered grafts, in contrast, remains significantly deficient, with only one relevant study identified thus far. Zhou et al. [201] conducted the first clinical trial on auricle cartilage regeneration for microtia treatment. They performed CT scans of the patient's unaffected ear, fabricated a morphologically bionic auricle scaffold using PCL, and implanted autologous cartilage cells into the scaffold before executing the transplantation. A 2.5-year follow-up ensued, ultimately revealing mature cartilage regeneration and aesthetically pleasing outcomes. However, the study only examined five cases and employed three distinct surgical procedures, failing to incorporate the intricate biomaterials and allogeneic cells utilized in numerous aforementioned studies. Consequently, conducting extensive clinical trials may encounter various challenges, including limited cell sources, long-term shape and mechanical stability concerns and biosafety issues. Moreover, many countries lack guidelines for clinical translation of 3D bioprinting [202]. Therefore, bionic 3D bioprinting may still have a considerable distance to traverse before achieving tangible clinical applications.

Declaration of competing interest

The authors declare that they have no known competing financial interests or personal relationships that could have appeared to influence the work reported in this paper.

Data availability

No data was used for the research described in the article.

Acknowledgments

This work was supported by the National Natural Science Foundation of China (No. 82272473 and 82202687)

Abbreviations

3D	Three dimension
ECM	Extracellular matrix
HA	Hyaluronic acid
GelMA	Gelatin methacrylate
HAMA	Hyaluronic acid methacrylate
PCL	Polycaprolactone
Ag	Agarose
MFCs	Meniscal fibrocartilage cells
PEGDA	Polyethylene glycol diacrylate
TGF-β1	Translational growth factor-β1
hMSCs	Human mesenchymal stem cells
hNCCs	Human nasal chondrocytes
hNTSCs	Human nasal turbinate stem cells
HUVECs	Umbilical vein endothelial cells
NHDF	Normal human dermal fibroblasts
MEW	Melt electrowriting
SLA	Stereo lithography appearance
DLP	Digital light processing
CSMA	Chondroitin methacrylate sulfate
VEGF	Vascular endothelial growth factor
FGF	Fibroblast growth factor
BMP	Bone morphogenetic protein
PDGF	Platelet-derived growth factor
IGF-1	Insulin growth factor
BMSCs	Bone marrow mesenchyml stem cells
PU	Polyurethane
GG	Gellan gum
GA	Glucosamine
SF-MA	Silk fibroin methacrylate
PVA	Poly(vinyl alcohol)
Alg	Alginate
SMSCs	Synovium-derived mesenchymal stem cells
KGN	Kartogenin
PLGA	Poly(lactic-*co*-glycolic acid
PDGF-BB	Platelet-derived growth factor-BB
GT	Gelatin
ADSCs	Adipose-derived stem cells

ACCs	Chondrocytes
PLA	Polylactic acid
SA	Sodium Alginate
CTGF	Connective tissue growth factor
IVD	Intervertebral disc

References

[1] Y. Wang, J. Zhang, W. Liang, X. Xiao, J. Zhang, J. Zhang, Z. Su, M. Liu, Y. Chen, C. Ji, Ear reconstruction with the combination of expanded skin flap and medpor framework: 20 Years of experience in a single center, Plast. Reconstr. Surg. 148 (4) (2021 Oct 1) 850–860.

[2] T. Nakamura, T. Sato, M. Araki, S. Ichihara, A. Nakada, M. Yoshitani, S. Itoi, M. Yamashita, S. Kanemaru, K. Omori, Y. Hori, K. Endo, Y. Inada, K. Hayakawa, In situ tissue engineering for tracheal reconstruction using a luminar remodeling type of artificial trachea, J. Thorac. Cardiovasc. Surg. 138 (4) (2009 Oct) 811–819.

[3] H. Li, Z. He, W. Li, J. Yao, C. Lyu, Y. Du, D. Xing, J. Lin, Exploring the mechanism of microfracture in the treatment of porcine full-thickness cartilage defect, Am. J. Sports Med. 51 (4) (2023 Mar) 1033–1046.

[4] L.H.N. Dang, N.T. Tran, J.S. Oh, T.Y. Kwon, K.B. Lee, Effect of bone morphogenetic protein-2 combined with microfracture for osteochondral defect of the talus in a rabbit model, Am. J. Sports Med. (2023 Apr 4), 3635465231162316.

[5] M. Snow, L. Middleton, S. Mehta, A. Roberts, R. Gray, J. Richardson, J.H. Kuiper, Active Consortium, A. Smith, S. White, S. Roberts, D. Griffiths, A. Mohammed, K. Moholkar, T. Ashraf, M. Green, J. Hutchinson, T. Bhullar, S. Chitnis, A. Shaw, L. van Niekerk, A. Hui, J.O. Drogset, G. Knutsen, M. McNicholas, M. Bowditch, D. Johnson, P. Turner, S. Chugh, N. Hunt, S. Ali, S. Palmer, A. Perry, A. Davidson, P. Hill, S. Deo, V. Satish, M. Radford, R. Langstaff, D. Houlihan-Burne, D. Spicer, P. Phaltankar, A. Hegab, D. Marsh, S. Cannon, T. Briggs, R. Pollock, R. Carrington, J. Skinner, G. Bentley, A. Price, P. Schranz, V. Mandalia, S. O'Brien, A randomized trial of autologous chondrocyte implantation versus alternative forms of surgical cartilage management in patients with a failed primary treatment for chondral or osteochondral defects in the knee, Am. J. Sports Med. 51 (2) (2023 Feb) 367–378.

[6] A. Pareek, P.J. Reardon, J.A. Macalena, B.A. Levy, M.J. Stuart, R.J. Williams 3rd, A.J. Krych, Osteochondral autograft transfer versus microfracture in the knee: a meta-analysis of prospective comparative studies at midterm, Arthroscopy 32 (10) (2016 Oct) 2118–2130.

[7] M. Ma, F. Zou, B. Abudureheman, F. Han, G. Xu, Y. Xie, K. Qiao, J. Peng, Y. Guan, H. Meng, Y. Zheng, Magnetic microcarriers with accurate localization and proliferation of mesenchymal stem cell for cartilage defects repairing, ACS Nano. 17 (7) (2023) 6373–6386.

[8] F. Daou, A. Cochis, M. Leigheb, L. Rimondini, Current advances in the regeneration of degenerated articular cartilage: a literature review on tissue engineering and its recent clinical translation, Materials 15 (1) (2021 Dec 21) 31.

[9] M. Samie, A.F. Khan, S.U. Rahman, H. Iqbal, M.A. Yameen, A.A. Chaudhry, H. A. Galeb, N.R. Halcovitch, J.G. Hardy, Drug/bioactive eluting chitosan composite foams for osteochondral tissue engineering, Int. J. Biol. Macromol. 229 (2023 Feb 28) 561–574.

[10] M. Guastaferro, L. Baldino, E. Reverchon, S. Cardea, Production of porous agarose-based structures: freeze-drying vs. Supercritical CO2 drying, Gels 7 (4) (2021 Nov 5) 198.

[11] K. Klimek, M. Tarczynska, W. Truszkiewicz, K. Gaweda, T.E.L. Douglas, G. Ginalska, Freeze-dried curdlan/whey protein isolate-based biomaterial as promising scaffold for matrix-associated autologous chondrocyte transplantation-A pilot in-vitro study, Cells 11 (2) (2022 Jan 14) 282.

[12] F. Han, Q. Yu, G. Chu, J. Li, Z. Zhu, Z. Tu, C. Liu, W. Zhang, R. Zhao, H. Mao, F. Han, B. Li, Multifunctional nanofibrous scaffolds with angle-ply microstructure and Co-delivery capacity promote partial repair and total replacement of intervertebral disc, Adv. Healthcare Mater. 11 (19) (2022 Oct), e2200895.

[13] F. Han, Q. Yu, G. Chu, J. Li, Z. Zhu, Z. Tu, C. Liu, W. Zhang, R. Zhao, H. Mao, F. Han, B. Li, Multifunctional nanofibrous scaffolds with angle-ply microstructure and Co-delivery capacity promote partial repair and total replacement of intervertebral disc, Adv. Healthcare Mater. 11 (19) (2022 Oct), e2200895.

[14] S. Ghadirian, S. Karbasi, Evaluation of the effects of halloysite nanotube on polyhydroxybutyrate - chitosan electrospun scaffolds for cartilage tissue engineering applications, Int. J. Biol. Macromol. 233 (2023 Apr 1), 123651.

[15] X. Li, X. Li, J. Yang, J. Lin, Y. Zhu, X. Xu, W. Cui, Living and injectable porous hydrogel microsphere with paracrine activity for cartilage regeneration, Small (2023 Jan 18), e2207211.

[16] Y. Yao, G. Wei, L. Deng, W. Cui, Visualizable and lubricating hydrogel microspheres via NanoPOSS for cartilage regeneration, Adv. Sci. (2023 Mar 27), e2207438.

[17] Y. Qu, S. He, S. Luo, J. Zhao, R. Liang, C. Liao, L. Zheng, Photocrosslinkable, injectable locust bean gum hydrogel induces chondrogenic differentiation of stem cells for cartilage regeneration, Adv. Healthcare Mater. (2023 Mar 7), e2203079.

[18] T. Wang, Y. Li, J. Liu, Y. Fang, W. Guo, Y. Liu, X. Li, G. Li, X. Wang, Z. Zheng, X. Wang, D.L. Kaplan, Intraarticularly injectable silk hydrogel microspheres with enhanced mechanical and structural stability to attenuate osteoarthritis, Biomaterials 286 (2022 Jul), 121611.

[19] Y. Chen, W. Xu, M. Shafiq, D. Song, T. Wang, Z. Yuan, X. Xie, X. Yu, Y. Shen, B. Sun, Y. Liu, X. Mo, Injectable nanofiber microspheres modified with metal phenolic networks for effective osteoarthritis treatment, Acta Biomater. 157 (2023 Feb) 593–608.

[20] Y. Xu, C. Chen, P.B. Hellwarth, X. Bao, Biomaterials for stem cell engineering and biomanufacturing, Bioact. Mater. 4 (2019 Dec 2) 366–379.

[21] J.E. Steele, How do we get there?, in: Bionics Symposium: Living Prototypes-The Key to New Technology [M] Routledge, NY, USA, 1960, pp. 55–60.

[22] C.W. Hull, Apparatus for production of three-dimensional objects by stereolithography: US5556590 A[P], 2020.

[23] D.R. Eyre, J.J. Wu, Collagen structure and cartilage matrix integrity, J. Rheumatol. Suppl. 43 (1995 Feb) 82–85.

[24] E.S. Mameri, S.P. Dasari, L.M. Fortier, F.G. Verdejo, S. Gursoy, A.B. Yanke, J. Chahla, Review of meniscus anatomy and biomechanics, Curr Rev Musculoskelet Med 15 (5) (2022 Oct) 323–335.

[25] T. Brindle, J. Nyland, D.L. Johnson, The meniscus: review of basic principles with application to surgery and rehabilitation, J. Athl. Train. 36 (2) (2001 Apr) 160–169.

[26] K. Martyniak, A. Lokshina, M.A. Cruz, M. Karimzadeh, R. Kemp, T.J. Kean, Biomaterial composition and stiffness as decisive properties of 3D bioprinted constructs for type II collagen stimulation, Acta Biomater. 152 (2022 Oct 15) 221–234.

[27] M. Chen, Z. Feng, W. Guo, D. Yang, S. Gao, Y. Li, S. Shen, Z. Yuan, B. Huang, Y. Zhang, M. Wang, X. Li, L. Hao, J. Peng, S. Liu, Y. Zhou, Q. Guo, PCL-MECM-Based hydrogel hybrid scaffolds and meniscal fibrochondrocytes promote whole meniscus regeneration in a rabbit meniscectomy model, ACS Appl. Mater. Interfaces 11 (44) (2019 Nov 6) 41626–41639.

[28] A. Vahdati, D.R. Wagner, Implant size and mechanical properties influence the failure of the adhesive bond between cartilage implants and native tissue in a finite element analysis, J. Biomech. 46 (9) (2013 May 31) 1554–1560.

[29] E. Stocco, A. Porzionato, E. De Rose, S. Barbon, R. De Caro, V. Macchi, Meniscus regeneration by 3D printing technologies: current advances and future perspectives, J. Tissue Eng. 13 (2022 Jan 25), 20417314211065860.

[30] G.K. Tan, J.J. Cooper-White, Interactions of meniscal cells with extracellular matrix molecules: towards the generation of tissue engineered menisci, Cell Adhes. Migrat. 5 (3) (2011 May-Jun) 220–226.

[31] O. Krupkova, L. Smolders, K. Wuertz-Kozak, J. Cook, A. Pozzi, The pathobiology of the meniscus: a comparison between the human and dog, Front. Vet. Sci. 5 (2018 Apr 16) 73.

[32] G. Bahcecioglu, B. Bilgen, N. Hasirci, V. Hasirci, Anatomical meniscus construct with zone specific biochemical composition and structural organization, Biomaterials 218 (2019 Oct), 119361.

[33] W. Guo, M. Chen, Z. Wang, Y. Tian, J. Zheng, S. Gao, Y. Li, Y. Zheng, X. Li, J. Huang, W. Niu, S. Jiang, C. Hao, Z. Yuan, Y. Zhang, M. Wang, Z. Wang, J. Peng, A. Wang, Y. Wang, X. Sui, W. Xu, L. Hao, X. Zheng, S. Liu, Q. Guo, 3D-printed cell-free PCL-MECM scaffold with biomimetic micro-structure and micro-environment to enhance in situ meniscus regeneration, Bioact. Mater. 6 (10) (2021 Mar 27) 3620–3633.

[34] J.M. Lee, W.L. Ng, W.Y. Yeong, Resolution and shape in bioprinting: strategizing towards complex tissue and organ printing, Appl. Phys. Rev. 6 (1) (2019).

[35] J.M. Lee, W.Y. Yeong, Design and printing strategies in 3D bioprinting of cell-hydrogels: a review, Adv. Healthcare Mater. 5 (22) (2016 Nov) 2856–2865.

[36] E.A. Makris, P. Hadidi, K.A. Athanasiou, The knee meniscus: structure-function, pathophysiology, current repair techniques, and prospects for regeneration, Biomaterials 32 (30) (2011 Oct) 7411–7431.

[37] H. Kurosawa, T. Fukubayashi, H. Nakajima, Load-bearing mode of the knee joint: physical behavior of the knee joint with or without menisci, Clin. Orthop. Relat. Res. 149 (1980 Jun) 283–290.

[38] K.A. Athanasiou, A. Agarwal, F.J. Dzida, Comparative study of the intrinsic mechanical properties of the human acetabular and femoral head cartilage, J. Orthop. Res. 12 (3) (1994 May) 340–349.

[39] S. Taheri, H.S. Ghazali, Z.S. Ghazali, A. Bhattacharyya, I. Noh, Progress in biomechanical stimuli on the cell-encapsulated hydrogels for cartilage tissue regeneration, Biomater. Res. 27 (1) (2023 Mar 20) 22.

[40] M.A. Stager, S.M. Thomas, N. Rotello-Kuri, K.A. Payne, M.D. Krebs, Polyelectrolyte complex hydrogels with controlled mechanics affect mesenchymal stem cell differentiation relevant to growth plate injuries, Macromol. Biosci. 22 (9) (2022 Sep), e2200126.

[41] Y.W. Chen, Y.H. Lin, T.L. Lin, K.A. Lee, M.H. Yu, M.Y. Shie, 3D-biofabricated chondrocyte-laden decellularized extracellular matrix-contained gelatin methacrylate auxetic scaffolds under cyclic tensile stimulation for cartilage regeneration, Biofabrication 15 (4) (2023 Jul 31).

[42] X. Zhou, T. Esworthy, S.J. Lee, S. Miao, H. Cui, M. Plesiniak, H. Fenniri, T. Webster, R.D. Rao, L.G. Zhang, 3D Printed scaffolds with hierarchical biomimetic structure for osteochondral regeneration, Nanomedicine 19 (2019 Jul) 58–70.

[43] J.H. Park, M. Ahn, S.H. Park, H. Kim, M. Bae, W. Park, S.J. Hollister, S.W. Kim, D. W. Cho, 3D bioprinting of a trachea-mimetic cellular construct of a clinically relevant size, Biomaterials 279 (2021 Dec), 121246.

[44] L. Zhang, J. Hu, K.A. Athanasiou, The role of tissue engineering in articular cartilage repair and regeneration, Crit. Rev. Biomed. Eng. 37 (1–2) (2009) 1–57.

[45] R. Machino, K. Matsumoto, D. Taniguchi, T. Tsuchiya, Y. Takeoka, Y. Taura, M. Moriyama, T. Tetsuo, S. Oyama, K. Takagi, T. Miyazaki, G. Hatachi, R. Doi, K. Shimoyama, N. Matsuo, N. Yamasaki, K. Nakayama, T. Nagayasu, Replacement of rat tracheas by layered, trachea-like, scaffold-free structures of human cells using a bio-3D printing system, Adv. Healthcare Mater. 8 (7) (2019 Apr), e1800983.

[46] W. Zhang, C. Ling, X. Li, R. Sheng, H. Liu, A. Zhang, Y. Jiang, J. Chen, Q. Yao, Cell-free biomimetic scaffold with cartilage extracellular matrix-like architectures for in situ inductive regeneration of osteochondral defects, ACS Biomater. Sci. Eng. 6 (12) (2020 Dec 14) 6917–6925.
[47] G. Haghiashtiani, K. Qiu, J.D. Zhingre Sanchez, Z.J. Fuenning, P. Nair, S. E. Ahlberg, P.A. Iaizzo, M.C. McAlpine, 3D printed patient-specific aortic root models with internal sensors for minimally invasive applications, Sci. Adv. 6 (35) (2020 Aug 28), eabb4641.
[48] B. Grigoryan, S.J. Paulsen, D.C. Corbett, D.W. Sazer, C.L. Fortin, A.J. Zaita, P. T. Greenfield, N.J. Calafat, J.P. Gounley, A.H. Ta, F. Johansson, A. Randles, J. E. Rosenkrantz, J.D. Louis-Rosenberg, P.A. Galie, K.R. Stevens, J.S. Miller, Multivascular networks and functional intravascular topologies within biocompatible hydrogels, Science 364 (6439) (2019 May 3) 458–464.
[49] Y. Yang, Z. Yu, X. Lu, J. Dai, C. Zhou, J. Yan, L. Wang, Z. Wang, J. Zang, Minimally invasive bioprinting for in situ liver regeneration, Bioact. Mater. 26 (2023 Mar 29) 465–477.
[50] J. Lee, H. Lee, E.J. Jin, D. Ryu, G.H. Kim, 3D bioprinting using a new photo-crosslinking method for muscle tissue restoration, NPJ Regen Med 8 (1) (2023 Mar 31) 18.
[51] J. Yang, K. Yang, W. Man, J. Zheng, Z. Cao, C.Y. Yang, K. Kim, S. Yang, Z. Hou, G. Wang, X. Wang, 3D bio-printed living nerve-like fibers refine the ecological niche for long-distance spinal cord injury regeneration, Bioact. Mater. 25 (2023 Feb 2) 160–175.
[52] M. Xie, J. Su, S. Zhou, J. Li, K. Zhang, Application of hydrogels as three-dimensional bioprinting ink for tissue engineering, Gels 9 (2) (2023 Jan 19) 88.
[53] B.N. Johnson, K.Z. Lancaster, G. Zhen, J. He, M.K. Gupta, Y.L. Kong, E.A. Engel, K.D. Krick, A. Ju, F. Meng, L.W. Enquist, X. Jia, M.C. McAlpine, 3D printed anatomical nerve regeneration pathways, Adv. Funct. Mater. 25 (39) (2015 Oct 21) 6205–6217.
[54] A. Lee, A.R. Hudson, D.J. Shiwarski, J.W. Tashman, T.J. Hinton, S. Yerneni, J. M. Bliley, P.G. Campbell, A.W. Feinberg, 3D bioprinting of collagen to rebuild components of the human heart, Science 365 (6452) (2019 Aug 2) 482–487.
[55] E. Kim, S. Choi, B. Kang, J. Kong, Y. Kim, W.H. Yoon, H.R. Lee, S. Kim, H.M. Kim, H. Lee, C. Yang, Y.J. Lee, M. Kang, T.Y. Roh, S. Jung, S. Kim, J.H. Ku, K. Shin, Creation of bladder assembloids mimicking tissue regeneration and cancer, Nature 588 (7839) (2020 Dec) 664–669.
[56] J.H. Kim, I. Kim, Y.J. Seol, I.K. Ko, J.J. Yoo, A. Atala, S.J. Lee, Neural cell integration into 3D bioprinted skeletal muscle constructs accelerates restoration of muscle function, Nat. Commun. 11 (1) (2020 Feb 24) 1025.
[57] M. Zhang, R. Lin, X. Wang, J. Xue, C. Deng, C. Feng, H. Zhuang, J. Ma, C. Qin, L. Wan, J. Chang, C. Wu, 3D printing of Haversian bone-mimicking scaffolds for multicellular delivery in bone regeneration, Sci. Adv. 6 (12) (2020 Mar 20) eaaz6725.
[58] M. Qiu, C. Li, Z. Cai, C. Li, K. Yang, N. Tulufu, B. Chen, L. Cheng, C. Zhuang, Z. Liu, J. Qi, W. Cui, L. Deng, 3D biomimetic calcified cartilaginous callus that induces type H vessels formation and osteoclastogenesis, Adv. Sci. (2023 Mar 31), e2207089.
[59] K.T. Lawlor, J.M. Vanslambrouck, J.W. Higgins, A. Chambon, K. Bishard, D. Arndt, P.X. Er, S.B. Wilson, S.E. Howden, K.S. Tan, F. Li, L.J. Hale, B. Shepherd, S. Pentoney, S.C. Presnell, A.E. Chen, M.H. Little, Cellular extrusion bioprinting improves kidney organoid reproducibility and conformation, Nat. Mater. 20 (2) (2021 Feb) 260–271.
[60] Z. Jian, T. Zhuang, T. Qinyu, P. Liqing, L. Kun, L. Xujiang, W. Diaodiao, Y. Zhen, J. Shuangpeng, S. Xiang, H. Jingxiang, L. Shuyun, H. Libo, T. Peifu, Y. Qi, G. Quanyi, 3D bioprinting of a biomimetic meniscal scaffold for application in tissue engineering, Bioact. Mater. 6 (6) (2020 Nov 30) 1711–1726.
[61] S. Sakai, A. Yoshii, S. Sakurai, K. Horii, O. Nagasuna, Silk fibroin nanofibers: a promising ink additive for extrusion three-dimensional bioprinting, Mater Today Bio 8 (2020 Sep 19), 100078.
[62] J. Wang, A. Goyanes, S. Gaisford, A.W. Basit, Stereolithographic (SLA) 3D printing of oral modified-release dosage forms, Int. J. Pharm. 503 (1–2) (2016 Apr 30) 207–212.
[63] W. Li, M. Wang, H. Ma, F.A. Chapa-Villarreal, A.O. Lobo, Y.S. Zhang, Stereolithography apparatus and digital light processing-based 3D bioprinting for tissue fabrication, iScience 26 (2) (2023 Jan 24), 106039.
[64] H. Quan, T. Zhang, H. Xu, S. Luo, J. Nie, X. Zhu, Photo-curing 3D printing technique and its challenges, Bioact. Mater. 5 (1) (2020 Jan 22) 110–115.
[65] S.A. Schoonraad, K.M. Fischenich, K.N. Eckstein, V. Crespo-Cuevas, L.M. Savard, A. Muralidharan, A.A. Tomaschke, A.C. Uzcategui, M.A. Randolph, R.R. McLeod, V.L. Ferguson, S.J. Bryant, Biomimetic and mechanically supportive 3D printed scaffolds for cartilage and osteochondral tissue engineering using photopolymers and digital light processing, Biofabrication 13 (4) (2021 Sep 16).
[66] X. Li, B. Liu, B. Pei, J. Chen, D. Zhou, J. Peng, X. Zhang, W. Jia, T. Xu, Inkjet bioprinting of biomaterials, Chem. Rev. 120 (19) (2020 Oct 14) 10793–10833.
[67] T. Xu, K.W. Binder, M.Z. Albanna, D. Dice, W. Zhao, J.J. Yoo, A. Atala, Hybrid printing of mechanically and biologically improved constructs for cartilage tissue engineering applications, Biofabrication 5 (1) (2013 Mar), 015001.
[68] X. Barceló, K.F. Eichholz, I.F. Gonçalves, O. Garcia, D.J. Kelly, Bioprinting of structurally organized meniscal tissue within anisotropic melt electrowritten scaffolds, Acta Biomater. 158 (2023 Mar 1) 216–227.
[69] G.H. Yang, M. Yeo, Y.W. Koo, G.H. Kim, 4D bioprinting: technological advances in biofabrication, Macromol. Biosci. 19 (5) (2019 May), e1800441.
[70] J.W. Boley, W.M. van Rees, C. Lissandrello, M.N. Horenstein, R.L. Truby, A. Kotikian, J.A. Lewis, L. Mahadevan, Shape-shifting structured lattices via multimaterial 4D printing, Proc. Natl. Acad. Sci. U. S. A. 116 (42) (2019 Oct 15) 20856–20862.
[71] I. Apsite, G. Stoychev, W. Zhang, D. Jehnichen, J. Xie, L. Ionov, Porous stimuli-responsive self-folding electrospun mats for 4D biofabrication, Biomacromolecules 18 (10) (2017 Oct 9) 3178–3184.
[72] M. Nadgorny, A. Ameli, Functional polymers and nanocomposites for 3D printing of smart structures and devices, ACS Appl. Mater. Interfaces 10 (21) (2018 May 30) 17489–17507.
[73] Y.S. Lui, W.T. Sow, L.P. Tan, Y. Wu, Y. Lai, H. Li, 4D printing and stimuli-responsive materials in biomedical aspects, Acta Biomater. 92 (2019 Jul 1) 19–36.
[74] C.D. Devillard, C.A. Mandon, S.A. Lambert, L.J. Blum, C.A. Marquette, Bioinspired multi-activities 4D printing objects: a new approach toward complex tissue engineering, Biotechnol. J. 13 (12) (2018 Dec), e1800098.
[75] M. Betsch, C. Cristian, Y.Y. Lin, A. Blaeser, J. Schöneberg, M. Vogt, E.M. Buhl, H. Fischer, D.F. Duarte Campos, Incorporating 4D into bioprinting: real-time magnetically directed collagen fiber alignment for generating complex multilayered tissues, Adv. Healthcare Mater. 7 (21) (2018 Nov), e1800894.
[76] N. Huebsch, C.J. Kearney, X. Zhao, J. Kim, C.A. Cezar, Z. Suo, D.J. Mooney, Ultrasound-triggered disruption and self-healing of reversibly cross-linked hydrogels for drug delivery and enhanced chemotherapy, Proc. Natl. Acad. Sci. U. S. A. 111 (27) (2014 Jul 8) 9762–9767.
[77] Y. Luo, X. Lin, B. Chen, X. Wei, Cell-laden four-dimensional bioprinting using near-infrared-triggered shape-morphing alginate/polydopamine bioinks, Biofabrication 11 (4) (2019 Sep 13), 045019.
[78] S.B. Gugulothu, K. Chatterjee, Visible light-based 4D-bioprinted tissue scaffold, ACS Macro Lett. (2023 Apr 1) 494–502.
[79] G.H. Yang, W. Kim, J. Kim, G. Kim, A skeleton muscle model using GelMA-based cell-aligned bioink processed with an electric-field assisted 3D/4D bioprinting, Theranostics 11 (1) (2021 Jan 1) 48–63.
[80] J.R. Clegg, A.M. Wagner, S.R. Shin, S. Hassan, A. Khademhosseini, N.A. Peppas, Modular fabrication of intelligent material-tissue interfaces for bioinspired and biomimetic devices, Prog. Mater. Sci. 106 (2019 Dec), 100589.
[81] P.J. Díaz-Payno, M. Kalogeropoulou, I. Muntz, E. Kingma, N. Kops, M. D'Este, G. H. Koenderink, L.E. Fratila-Apachitei, G.J.V.M. van Osch, A.A. Zadpoor, Swelling-dependent shape-based transformation of a human mesenchymal stromal cells-laden 4D bioprinted construct for cartilage tissue engineering, Adv. Healthcare Mater. 12 (2) (2023 Jan), e2201891.
[82] S.H. Kim, Y.B. Seo, Y.K. Yeon, Y.J. Lee, H.S. Park, M.T. Sultan, J.M. Lee, J.S. Lee, O.J. Lee, H. Hong, H. Lee, O. Ajiteru, Y.J. Suh, S.H. Song, K.H. Lee, C.H. Park, 4D-bioprinted silk hydrogels for tissue engineering, Biomaterials 260 (2020 Nov), 120281.
[83] A. Ding, O. Jeon, D. Cleveland, K.L. Gasvoda, D. Wells, S.J. Lee, E. Alsberg, Jammed micro-flake hydrogel for four-dimensional living cell bioprinting, Adv. Mater. 34 (15) (2022 Apr), e2109394.
[84] J. Chakraborty, J. Fernández-Pérez, K.A. van Kampen, S. Roy, T. Ten Brink, C. Mota, S. Ghosh, L. Moroni, Development of a biomimetic arch-like 3D bioprinted construct for cartilage regeneration using gelatin methacryloyl and silk fibroin-gelatin bioinks, Biofabrication 15 (3) (2023 Apr 14).
[85] J. Zeng, L. Jia, D. Wang, Z. Chen, W. Liu, Q. Yang, X. Liu, H. Jiang, Bacterial nanocellulose-reinforced gelatin methacryloyl hydrogel enhances biomechanical property and glycosaminoglycan content of 3D-bioprinted cartilage, Int J Bioprint 9 (1) (2022 Oct 29) 631, https://doi.org/10.18063/ijb.v9i1.631.
[86] K. Flégeau, A. Puiggali-Jou, M. Zenobi-Wong, Cartilage tissue engineering by extrusion bioprinting utilizing porous hyaluronic acid microgel bioinks, Biofabrication 14 (3) (2022 May 13).
[87] J. Hauptstein, L. Forster, A. Nadernezhad, J. Groll, J. Teßmar, T. Blunk, Tethered TGF-β1 in a hyaluronic acid-based bioink for bioprinting cartilaginous tissues, Int. J. Mol. Sci. 23 (2) (2022 Jan 15) 924.
[88] M.C. Decarli, A. Seijas-Gamardo, F. Morgan, P. Wieringa, M.B. Baker, J.V.L. Silva, Â.M. Moraes, L. Moroni, C. Mota, Bioprinting of stem cell spheroids followed by post-printing chondrogenic differentiation for cartilage tissue engineering, Adv. Healthcare Mater. (2023 Apr 14), e2203021.
[89] Y. Chen, Y. Chen, X. Xiong, R. Cui, G. Zhang, C. Wang, D. Xiao, S. Qu, J. Weng, Hybridizing gellan/alginate and thixotropic magnesium phosphate-based hydrogel scaffolds for enhanced osteochondral repair, Mater Today Bio 14 (2022 Apr 13), 100261.
[90] M.C. Decarli, A. Seijas-Gamardo, F. Morgan, P. Wieringa, M.B. Baker, J.V.L. Silva, Â.M. Moraes, L. Moroni, C. Mota, Bioprinting of stem cell spheroids followed by post-printing chondrogenic differentiation for cartilage tissue engineering, Adv. Healthcare Mater. (2023 Apr 14), e2203021.
[91] H. Hong, Y.B. Seo, D.Y. Kim, J.S. Lee, Y.J. Lee, H. Lee, O. Ajiteru, M.T. Sultan, O. J. Lee, S.H. Kim, C.H. Park, Digital light processing 3D printed silk fibroin hydrogel for cartilage tissue engineering, Biomaterials 232 (2020 Feb), 119679.
[92] Y.P. Singh, A. Bandyopadhyay, B.B. Mandal, 3D bioprinting using cross-linker-free silk-gelatin bioink for cartilage tissue engineering, ACS Appl. Mater. Interfaces 11 (37) (2019 Sep 18) 33684–33696.
[93] Á. Serrano-Aroca, A. Cano-Vicent, I. Sabater, R. Serra, M. El-Tanani, A. Aljabali, M.M. Tambuwala, Y.K. Mishra, Scaffolds in the microbial resistant era: fabrication, materials, properties and tissue engineering applications, Mater Today Bio 16 (2022 Aug 30), 100412.
[94] X. Zhang, Y. Liu, C. Luo, C. Zhai, Z. Li, Y. Zhang, T. Yuan, S. Dong, J. Zhang, W. Fan, Crosslinker-free silk/decellularized extracellular matrix porous bioink for 3D bioprinting-based cartilage tissue engineering, Mater. Sci. Eng., C 118 (2021 Jan), 111388.
[95] Y. Huang, X. Meng, Z. Zhou, W. Zhu, X. Chen, Y. He, N. He, X. Han, D. Zhou, X. Duan, P.M. Vadgama, H. Liu, A naringin-derived bioink enhances the shape

fidelity of 3D bioprinting and efficiency of cartilage defect repair, J. Mater. Chem. B 10 (36) (2022 Sep 21) 7030–7044.
[96] S.W. Kim, D.Y. Kim, H.H. Roh, H.S. Kim, J.W. Lee, K.Y. Lee, Three-dimensional bioprinting of cell-laden constructs using polysaccharide-based self-healing hydrogels, Biomacromolecules 20 (5) (2019 May 13) 1860–1866.
[97] Y. Ge, Y. Li, Z. Wang, L. Li, H. Teng, Q. Jiang, Effects of mechanical compression on chondrogenesis of human synovium-derived mesenchymal stem cells in agarose hydrogel, Front. Bioeng. Biotechnol. 9 (2021 Jul 19), 697281.
[98] M. Li, D. Sun, J. Zhang, Y. Wang, Q. Wei, Y. Wang, Application and development of 3D bioprinting in cartilage tissue engineering, Biomater. Sci. 10 (19) (2022 Sep 27) 5430–5458.
[99] S. Sang, X. Mao, Y. Cao, Z. Liu, Z. Shen, M. Li, W. Jia, Z. Guo, Z. Wang, C. Xiang, L. Sun, 3D bioprinting using synovium-derived MSC-laden photo-cross-linked ECM bioink for cartilage regeneration, ACS Appl. Mater. Interfaces 15 (7) (2023) 8895–8913.
[100] Z. Terzopoulou, A. Zamboulis, I. Koumentakou, G. Michailidou, M.J. Noordam, D. N. Bikiaris, Biocompatible synthetic polymers for tissue engineering purposes, Biomacromolecules 23 (5) (2022 May 9) 1841–1863, https://doi.org/10.1021/acs.biomac.2c00047. Epub 2022 Apr 19. PMID: 35438479.
[101] Z.Z. Zhang, S.J. Wang, J.Y. Zhang, W.B. Jiang, A.B. Huang, Y.S. Qi, J.X. Ding, X. S. Chen, D. Jiang, J.K. Yu, 3D-Printed poly(ε-caprolactone) scaffold augmented with mesenchymal stem cells for total meniscal substitution: a 12- and 24-week animal study in a rabbit model, Am. J. Sports Med. 45 (7) (2017 Jun) 1497–1511.
[102] Z.Z. Zhang, D. Jiang, J.X. Ding, S.J. Wang, L. Zhang, J.Y. Zhang, Y.S. Qi, X. S. Chen, J.K. Yu, Role of scaffold mean pore size in meniscus regeneration, Acta Biomater. 43 (2016 Oct 1) 314–326.
[103] Z. Abpeikar, M. Javdani, S.A. Mirzaei, A. Alizadeh, L. Moradi, M. Soleimannejad, S. Bonakdar, S. Asadpour, Macroporous scaffold surface modified with biological macromolecules and piroxicam-loaded gelatin nanofibers toward meniscus cartilage repair, Int. J. Biol. Macromol. 183 (2021 Jul 31) 1327–1345, https://doi.org/10.1016/j.ijbiomac.2021.04.151. Epub 2021 Apr 29. PMID: 33932422.
[104] Z. Abpeikar, M. Javdani, A. Alizadeh, P. Khosravian, L. Tayebi, S. Asadpour, Development of meniscus cartilage using polycaprolactone and decellularized meniscus surface modified by gelatin, hyaluronic acid biomacromolecules: a rabbit model, Int. J. Biol. Macromol. 213 (2022 Jul 31) 498–515.
[105] S. Gupta, A. Sharma, J. Vasantha Kumar, V. Sharma, P.K. Gupta, R.S. Verma, Meniscal tissue engineering via 3D printed PLA monolith with carbohydrate based self-healing interpenetrating network hydrogel, Int. J. Biol. Macromol. 162 (2020 Nov 1) 1358–1371.
[106] X. Lan, Y. Boluk, A.B. Adesida, 3D bioprinting of hyaline cartilage using nasal chondrocytes, Ann. Biomed. Eng. (2023 Mar 23).
[107] X. Ren, F. Wang, C. Chen, X. Gong, L. Yin, L. Yang, Engineering zonal cartilage through bioprinting collagen type II hydrogel constructs with biomimetic chondrocyte density gradient, BMC Muscoskel. Disord. 17 (2016 Jul 20) 301.
[108] S. Rhee, J.L. Puetzer, B.N. Mason, C.A. Reinhart-King, L.J. Bonassar, 3D bioprinting of spatially heterogeneous collagen constructs for cartilage tissue engineering, ACS Biomater. Sci. Eng. 2 (10) (2016 Oct 10) 1800–1805.
[109] Y. Luo, X. Wei, P. Huang, 3D bioprinting of hydrogel-based biomimetic microenvironments, J. Biomed. Mater. Res. B Appl. Biomater. 107 (5) (2019 Jul) 1695–1705.
[110] X. Lan, Z. Ma, A.R.A. Szojka, M. Kunze, A. Mulet-Sierra, M.J. Vyhlidal, Y. Boluk, A.B. Adesida, TEMPO-oxidized cellulose nanofiber-alginate hydrogel as a bioink for human meniscus tissue engineering, Front. Bioeng. Biotechnol. 9 (2021 Nov 5), 766399.
[111] X. Dong, I.D. Premaratne, J.L. Bernstein, A. Samadi, A.J. Lin, Y. Toyoda, J. Kim, L. J. Bonassar, J.A. Spector, Three-dimensional-printed external scaffolds mitigate loss of volume and topography in engineered elastic cartilage constructs, Cartilage 13 (2_suppl) (2021 Dec) 1780S–1789S.
[112] X. Xie, S. Wu, S. Mou, N. Guo, Z. Wang, J. Sun, Microtissue-based bioink as a chondrocyte microshelter for DLP bioprinting, Adv. Healthcare Mater. 11 (22) (2022 Nov), e2201877.
[113] R. Zheng, D. Song, Y. Ding, B. Sun, C. Lu, X. Mo, H. Xu, Y. Liu, J. Wu, A comparative study on various cell sources for constructing tissue-engineered meniscus, Front. Bioeng. Biotechnol. 11 (2023 Mar 16), 1128762, https://doi.org/10.3389/fbioe.2023.1128762. PMID: 37008037; PMCID: PMC10061001.
[114] C. Zhang, G. Wang, H. Lin, Y. Shang, N. Liu, Y. Zhen, Y. An, Cartilage 3D bioprinting for rhinoplasty using adipose-derived stem cells as seed cells: review and recent advances, Cell Prolif. 56 (4) (2023 Apr), e13417.
[115] Y. Liu, L. Peng, L. Li, C. Huang, K. Shi, X. Meng, P. Wang, M. Wu, L. Li, H. Cao, K. Wu, Q. Zeng, H. Pan, W.W. Lu, L. Qin, C. Ruan, X. Wang, 3D-bioprinted BMSC-laden biomimetic multiphasic scaffolds for efficient repair of osteochondral defects in an osteoarthritic rat model, Biomaterials 279 (2021 Dec), 121216.
[116] K. von der Mark, V. Gauss, H. von der Mark, P. Müller, Relationship between cell shape and type of collagen synthesised as chondrocytes lose their cartilage phenotype in culture, Nature 267 (5611) (1977 Jun 9) 531–532.
[117] C. Cournil-Henrionnet, C. Huselstein, Y. Wang, L. Galois, D. Mainard, V. Decot, P. Netter, J.F. Stoltz, S. Muller, P. Gillet, A. Watrin-Pinzano, Phenotypic analysis of cell surface markers and gene expression of human mesenchymal stem cells and chondrocytes during monolayer expansion, Biorheology 45 (3–4) (2008) 513–526.
[118] A.J. Friedenstein, R.K. Chailakhjan, K.S. Lalykina, The development of fibroblast colonies in monolayer cultures of Guinea-pig bone marrow and spleen cells, Cell Tissue Kinet. 3 (4) (1970 Oct) 393–403.
[119] C. De Bari, F. Dell'Accio, P. Tylzanowski, F.P. Luyten, Multipotent mesenchymal stem cells from adult human synovial membrane, Arthritis Rheum. 44 (8) (2001 Aug) 1928–1942.
[120] E.A. Jones, A. English, K. Henshaw, S.E. Kinsey, A.F. Markham, P. Emery, D. McGonagle, Enumeration and phenotypic characterization of synovial fluid multipotential mesenchymal progenitor cells in inflammatory and degenerative arthritis, Arthritis Rheum. 50 (3) (2004 Mar) 817–827.
[121] S. Gronthos, M. Mankani, J. Brahim, P.G. Robey, S. Shi, Postnatal human dental pulp stem cells (DPSCs) in vitro and in vivo, Proc. Natl. Acad. Sci. U. S. A. 97 (25) (2000 Dec 5) 13625–13630.
[122] A. Erices, P. Conget, J.J. Minguell, Mesenchymal progenitor cells in human umbilical cord blood, Br. J. Haematol. 109 (1) (2000 Apr) 235–242.
[123] K. Pelttari, A. Winter, E. Steck, K. Goetzke, T. Hennig, B.G. Ochs, T. Aigner, W. Richter, Premature induction of hypertrophy during in vitro chondrogenesis of human mesenchymal stem cells correlates with calcification and vascular invasion after ectopic transplantation in SCID mice, Arthritis Rheum. 54 (10) (2006 Oct) 3254–3266.
[124] J. Zhang, E. Wehrle, P. Adamek, G.R. Paul, X.H. Qin, M. Rubert, R. Müller, Optimization of mechanical stiffness and cell density of 3D bioprinted cell-laden scaffolds improves extracellular matrix mineralization and cellular organization for bone tissue engineering, Acta Biomater. 114 (2020 Sep 15) 307–322.
[125] O. Messaoudi, C. Henrionnet, K. Bourge, D. Loeuille, P. Gillet, A. Pinzano, Stem cells and extrusion 3D printing for hyaline cartilage engineering, Cells 10 (1) (2020 Dec 22) 2.
[126] O. Basal, O. Ozmen, A.M. Deliormanli, Effect of polycaprolactone scaffolds containing different weights of graphene on healing in large osteochondral defect model, J. Biomater. Sci. Polym. Ed. 33 (9) (2022 Jun) 1123–1139.
[127] D. Kilian, S. Cometta, A. Bernhardt, R. Taymour, J. Golde, T. Ahlfeld, J. Emmermacher, M. Gelinsky, A. Lode, Core-shell bioprinting as a strategy to apply differentiation factors in a spatially defined manner inside osteochondral tissue substitutes, Biofabrication (1) (2022 Jan 6) 14.
[128] Z. Yang, F. Cao, H. Li, S. He, T. Zhao, H. Deng, J. Li, Z. Sun, C. Hao, J. Xu, Q. Guo, S. Liu, W. Guo, Microenvironmentally optimized 3D-printed TGFβ-functionalized scaffolds facilitate endogenous cartilage regeneration in sheep, Acta Biomater. 150 (2022 Sep 15) 181–198.
[129] B. Wang, P.J. Díaz-Payno, D.C. Browe, F.E. Freeman, J. Nulty, R. Burdis, D. J. Kelly, Affinity-bound growth factor within sulfated interpenetrating network bioinks for bioprinting cartilaginous tissues, Acta Biomater. 128 (2021 Jul 1) 130–142.
[130] J. Jose, S. Sultan, N. Kalarikkal, S. Thomas, A.P. Mathew, Fabrication and functionalization of 3D-printed soft and hard scaffolds with growth factors for enhanced bioactivity, RSC Adv. 10 (62) (2020 Oct 14) 37928–37937.
[131] U.A. Gurkan, R. El Assal, S.E. Yildiz, Y. Sung, A.J. Trachtenberg, W.P. Kuo, U. Demirci, Engineering anisotropic biomimetic fibrocartilage microenvironment by bioprinting mesenchymal stem cells in nanoliter gel droplets, Mol. Pharm. 11 (7) (2014 Jul 7) 2151–2159.
[132] A.C. Daly, P. Pitacco, J. Nulty, G.M. Cunniffe, D.J. Kelly, 3D printed microchannel networks to direct vascularisation during endochondral bone repair, Biomaterials 162 (2018 Apr) 34–46.
[133] I. Mayoral, E. Bevilacqua, G. Gómez, A. Hmadcha, I. González-Loscertales, E. Reina, J. Sotelo, A. Domínguez, P. Pérez-Alcántara, Y. Smani, P. González-Puertas, A. Mendez, S. Uribe, T. Smani, A. Ordoñez, I. Valverde, Tissue engineered in-vitro vascular patch fabrication using hybrid 3D printing and electrospinning, Mater Today Bio 14 (2022 Apr 14), 100252.
[134] P. Wei, Y. Xu, Y. Gu, Q. Yao, J. Li, L. Wang, IGF-1-releasing PLGA nanoparticles modified 3D printed PCL scaffolds for cartilage tissue engineering, Drug Deliv. 27 (1) (2020 Dec) 1106–1114.
[135] M. Beudert, L. Hahn, A.H.C. Horn, N. Hauptstein, H. Sticht, L. Meinel, R. Luxenhofer, M. Gutmann, T. Lühmann, Merging bioresponsive release of insulin-like growth factor I with 3D printable thermogelling hydrogels, J. Contr. Release 347 (2022 Jul) 115–126.
[136] Y. Endo, M. Samandari, M. Karvar, A. Mostafavi, J. Quint, C. Rinoldi, I.K. Yazdi, W. Swieszkowski, J. Mauney, S. Agarwal, A. Tamayol, I. Sinha, Aerobic exercise and scaffolds with hierarchical porosity synergistically promote functional recovery post volumetric muscle loss, Biomaterials (2023 Feb 17), 122058, 296.
[137] E.S. Mameri, S.P. Dasari, L.M. Fortier, F.G. Verdejo, S. Gursoy, A.B. Yanke, J. Chahla, Review of meniscus anatomy and biomechanics, Curr Rev Musculoskelet Med 15 (5) (2022 Oct) 323–335.
[138] F. Amiri, M. Babaei, N. Jamshidi, M. Agheb, M. Rafienia, M. Kazemi, Fabrication and assessment of a novel hybrid scaffold consisted of polyurethane-gellan gum-hyaluronic acid-glucosamine for meniscus tissue engineering, Int. J. Biol. Macromol. 203 (2022 Apr 1) 610–622.
[139] J.B. Costa, J. Park, A.M. Jorgensen, J. Silva-Correia, R.L. Reis, J.M. Oliveira, A. Atala, J.J. Yoo, S.J. Lee, 3D bioprinted highly elastic hybrid constructs for advanced fibrocartilaginous tissue regeneration, Chem. Mater. 32 (19) (2020 Oct 13) 8733–8746.
[140] J. Lu, J. Huang, J. Jin, C. Xie, B. Xue, J. Lai, B. Cheng, L. Li, Q. Jiang, The design and characterization of a strong bio-ink for meniscus regeneration, Int J Bioprint 8 (4) (2022 Aug 8) 600.
[141] M. Chen, Z. Feng, W. Guo, D. Yang, S. Gao, Y. Li, S. Shen, Z. Yuan, B. Huang, Y. Zhang, M. Wang, X. Li, L. Hao, J. Peng, S. Liu, Y. Zhou, Q. Guo, PCL-MECM-Based hydrogel hybrid scaffolds and meniscal fibrochondrocytes promote whole meniscus regeneration in a rabbit meniscectomy model, ACS Appl. Mater. Interfaces 11 (44) (2019 Nov 6) 41626–41639.
[142] Z. Li, N. Wu, J. Cheng, M. Sun, P. Yang, F. Zhao, J. Zhang, X. Duan, X. Fu, J. Zhang, X. Hu, H. Chen, Y. Ao, Biomechanically, structurally and functionally meticulously tailored polycaprolactone/silk fibroin scaffold for meniscus regeneration, Theranostics 10 (11) (2020 Apr 6) 5090–5106.

[143] H. Li, Z. Liao, Z. Yang, C. Gao, L. Fu, P. Li, T. Zhao, F. Cao, W. Chen, Z. Yuan, X. Sui, S. Liu, Q. Guo, 3D printed poly(ε-caprolactone)/meniscus extracellular matrix composite scaffold functionalized with kartogenin-releasing PLGA microspheres for meniscus tissue engineering, Front. Bioeng. Biotechnol. 9 (2021 Apr 30), 662381.
[144] L. Hao, Z. Tianyuan, Y. Zhen, C. Fuyang, W. Jiang, Y. Zineng, D. Zhengang, L. Shuyun, H. Chunxiang, Y. Zhiguo, G. Quanyi, Biofabrication of cell-free dual drug-releasing biomimetic scaffolds for meniscal regeneration, Biofabrication 14 (1) (2021 Oct 18).
[145] B. Xu, J. Ye, B.S. Fan, X. Wang, J.Y. Zhang, S. Song, Y. Song, W.B. Jiang, X. Wang, J.K. Yu, Protein-spatiotemporal partition releasing gradient porous scaffolds and anti-inflammatory and antioxidant regulation remodel tissue engineered anisotropic meniscus, Bioact. Mater. 20 (2022 May 30) 194–207, https://doi.org/10.1016/j.bioactmat.2022.05.019. PMID: 35702607; PMCID: PMC9160676.
[146] Y. Sun, Y. Zhang, Q. Wu, F. Gao, Y. Wei, Y. Ma, W. Jiang, K. Dai, 3D-bioprinting ready-to-implant anisotropic menisci recapitulate healthy meniscus phenotype and prevent secondary joint degeneration, Theranostics 11 (11) (2021 Mar 5) 5160–5173.
[147] S. Chae, S.S. Lee, Y.J. Choi, D.H. Hong, G. Gao, J.H. Wang, D.W. Cho, 3D cell-printing of biocompatible and functional meniscus constructs using meniscus-derived bioink, Biomaterials 267 (2021 Jan), 120466.
[148] I.F. Cengiz, F.R. Maia, A. da Silva Morais, J. Silva-Correia, H. Pereira, R. F. Canadas, J. Espregueira-Mendes, I.K. Kwon, R.L. Reis, J.M. Oliveira, Entrapped in cage (EiC) scaffolds of 3D-printed polycaprolactone and porous silk fibroin for meniscus tissue engineering, Biofabrication 12 (2) (2020 Mar 13), 025028.
[149] E.B. Hunziker, T.M. Quinn, H.J. Häuselmann, Quantitative structural organization of normal adult human articular cartilage, Osteoarthritis Cartilage 10 (7) (2002 Jul) 564–572.
[150] S.L. Ding, X. Liu, X.Y. Zhao, K.T. Wang, W. Xiong, Z.L. Gao, C.Y. Sun, M.X. Jia, C. Li, Q. Gu, M.Z. Zhang, Microcarriers in application for cartilage tissue engineering: recent progress and challenges, Bioact. Mater. 17 (2022 Jan 25) 81–108.
[151] X. Yang, Z. Lu, H. Wu, W. Li, L. Zheng, J. Zhao, Collagen-alginate as bioink for three-dimensional (3D) cell printing based cartilage tissue engineering, Mater. Sci. Eng., C 83 (2018 Feb 1) 195–201.
[152] P. Li, L. Fu, Z. Liao, Y. Peng, C. Ning, C. Gao, D. Zhang, X. Sui, Y. Lin, S. Liu, C. Hao, Q. Guo, Chitosan hydrogel/3D-printed poly(ε-caprolactone) hybrid scaffold containing synovial mesenchymal stem cells for cartilage regeneration based on tetrahedral framework nucleic acid recruitment, Biomaterials 278 (2021 Nov), 121131.
[153] Q. Li, S. Xu, Q. Feng, Q. Dai, L. Yao, Y. Zhang, H. Gao, H. Dong, D. Chen, X. Cao, 3D printed silk-gelatin hydrogel scaffold with different porous structure and cell seeding strategy for cartilage regeneration, Bioact. Mater. 6 (10) (2021 Mar 19) 3396–3410.
[154] M. Chen, Y. Li, S. Liu, Z. Feng, H. Wang, D. Yang, W. Guo, Z. Yuan, S. Gao, Y. Zhang, K. Zha, B. Huang, F. Wei, X. Sang, Q. Tian, X. Yang, X. Sui, Y. Zhou, Y. Zheng, Q. Guo, Hierarchical macro-microporous WPU-ECM scaffolds combined with microfracture promote in situ articular cartilage regeneration in rabbits, Bioact. Mater. 6 (7) (2020 Dec 22) 1932–1944.
[155] W. Shi, M. Sun, X. Hu, B. Ren, J. Cheng, C. Li, X. Duan, X. Fu, J. Zhang, H. Chen, Y. Ao, Structurally and functionally optimized silk-fibroin-gelatin scaffold using 3D printing to repair cartilage injury in vitro and in vivo, Adv. Mater. 29 (29) (2017 Aug).
[156] D. Martínez-Moreno, D. Venegas-Bustos, G. Rus, P. Gálvez-Martín, G. Jiménez, J. A. Marchal, Chondro-inductive b-TPUe-based functionalized scaffolds for application in cartilage tissue engineering, Adv. Healthcare Mater. 11 (19) (2022 Oct), e2200251.
[157] C. Antich, J. de Vicente, G. Jiménez, C. Chocarro, E. Carrillo, E. Montañez, P. Gálvez-Martín, J.A. Marchal, Bio-inspired hydrogel composed of hyaluronic acid and alginate as a potential bioink for 3D bioprinting of articular cartilage engineering constructs, Acta Biomater. 106 (2020 Apr 1) 114–123.
[158] L. Gong, J. Li, J. Zhang, Z. Pan, Y. Liu, F. Zhou, Y. Hong, Y. Hu, Y. Gu, H. Ouyang, X. Zou, S. Zhang, An interleukin-4-loaded bi-layer 3D printed scaffold promotes osteochondral regeneration, Acta Biomater. 117 (2020 Nov) 246–260.
[159] J. Gao, X. Ding, X. Yu, X. Chen, X. Zhang, S. Cui, J. Shi, J. Chen, L. Yu, S. Chen, J. Ding, Cell-free bilayered porous scaffolds for osteochondral regeneration fabricated by continuous 3D-printing using nascent physical hydrogel as ink, Adv. Healthcare Mater. 10 (3) (2021 Feb), e2001404.
[160] J. Idaszek, M. Costantini, T.A. Karlsen, J. Jaroszewicz, C. Colosi, S. Testa, E. Fornetti, S. Bernardini, M. Seta, K. Kasarełło, R. Wrzesień, S. Cannata, A. Barbetta, C. Gargioli, J.E. Brinchman, W. Święszkowski, 3D bioprinting of hydrogel constructs with cell and material gradients for the regeneration of full-thickness chondral defect using a microfluidic printing head, Biofabrication 11 (4) (2019 Jul 1), 044101.
[161] Y. Han, M. Lian, B. Sun, B. Jia, Q. Wu, Z. Qiao, K. Dai, Preparation of high precision multilayer scaffolds based on Melt Electro-Writing to repair cartilage injury, Theranostics 10 (22) (2020 Aug 13) 10214–10230.
[162] Y. Han, M. Lian, B. Sun, B. Jia, Q. Wu, Z. Qiao, K. Dai, Preparation of high precision multilayer scaffolds based on Melt Electro-Writing to repair cartilage injury, Theranostics 10 (22) (2020 Aug 13) 10214–10230.
[163] A.C. Gelber, M.C. Hochberg, L.A. Mead, N.Y. Wang, F.M. Wigley, M.J. Klag, Joint injury in young adults and risk for subsequent knee and hip osteoarthritis, Ann. Intern. Med. 133 (5) (2000 Sep 5) 321–328.
[164] Q. Li, H. Yu, F. Zhao, C. Cao, T. Wu, Y. Fan, Y. Ao, X. Hu, 3D printing of microenvironment-specific bioinspired and exosome-reinforced hydrogel scaffolds for efficient cartilage and subchondral bone regeneration, Adv. Sci. 10 (26) (2023 Sep), e2303650.
[165] T. Guo, M. Noshin, H.B. Baker, E. Taskoy, S.J. Meredith, Q. Tang, J.P. Ringel, M. J. Lerman, Y. Chen, J.D. Packer, J.P. Fisher, 3D printed biofunctionalized scaffolds for microfracture repair of cartilage defects, Biomaterials 185 (2018 Dec) 219–231.
[166] B.K. Jung, J.Y. Kim, Y.S. Kim, T.S. Roh, A. Seo, K.H. Park, J.H. Shim, I.S. Yun, Ideal scaffold design for total ear reconstruction using a three-dimensional printing technique, J. Biomed. Mater. Res. B Appl. Biomater. 107 (4) (2019 May) 1295–1303.
[167] S. Liu, Q. Hu, Z. Shen, S. Krishnan, H. Zhang, M. Ramalingam, 3D printing of self-standing and vascular supportive multimaterial hydrogel structures for organ engineering, Biotechnol. Bioeng. 119 (1) (2022 Jan) 118–133.
[168] Q. Gao, X. Niu, L. Shao, L. Zhou, Z. Lin, A. Sun, J. Fu, Z. Chen, J. Hu, Y. Liu, Y. He, 3D printing of complex GelMA-based scaffolds with nanoclay, Biofabrication 11 (3) (2019 Apr 5), 035006.
[169] N. Bhamare, K. Tardalkar, P. Parulekar, A. Khadilkar, M. Joshi, 3D printing of human ear pinna using cartilage specific ink, Biomed. Mater. (5) (2021 Aug 3) 16.
[170] R. Yuan, K. Wu, Q. Fu, 3D printing of all-regenerated cellulose material with truly 3D configuration: the critical role of cellulose microfiber, Carbohydr. Polym. 294 (2022 Oct 15), 119784.
[171] Y.P. Singh, A. Bandyopadhyay, B.B. Mandal, 3D bioprinting using cross-linker-free silk-gelatin bioink for cartilage tissue engineering, ACS Appl. Mater. Interfaces 11 (37) (2019 Sep 18) 33684–33696.
[172] D.O. Visscher, H. Lee, P.P.M. van Zuijlen, M.N. Helder, A. Atala, J.J. Yoo, S.J. Lee, A photo-crosslinkable cartilage-derived extracellular matrix bioink for auricular cartilage tissue engineering, Acta Biomater. 121 (2021 Feb) 193–203.
[173] Y. Chen, J. Zhang, X. Liu, S. Wang, J. Tao, Y. Huang, W. Wu, Y. Li, K. Zhou, X. Wei, S. Chen, X. Li, X. Xu, L. Cardon, Z. Qian, M. Gou, Noninvasive in vivo 3D bioprinting, Sci. Adv. 6 (23) (2020 Jun 5), eaba7406.
[174] L. Zhang, W. Lee, X. Li, Y. Jiang, N.X. Fang, G. Dai, Y. Liu, 3D direct printing of mechanical and biocompatible hydrogel meta-structures, Bioact. Mater. 10 (2021 Sep 9) 48–55.
[175] P. Tang, P. Song, Z. Peng, B. Zhang, X. Gui, Y. Wang, X. Liao, Z. Chen, Z. Zhang, Y. Fan, Z. Li, Y. Cen, C. Zhou, Chondrocyte-laden GelMA hydrogel combined with 3D printed PLA scaffolds for auricle regeneration, Mater. Sci. Eng., C 130 (2021 Nov), 112423.
[176] H.W. Kang, S.J. Lee, I.K. Ko, C. Kengla, J.J. Yoo, A. Atala, A 3D bioprinting system to produce human-scale tissue constructs with structural integrity, Nat. Biotechnol. 34 (3) (2016 Mar) 312–319.
[177] L. Jia, Y. Hua, J. Zeng, W. Liu, D. Wang, G. Zhou, X. Liu, H. Jiang, Bioprinting and regeneration of auricular cartilage using a bioactive bioink based on microporous photocrosslinkable acellular cartilage matrix, Bioact. Mater. 16 (2022 Mar 3) 66–81.
[178] J.S. Lee, J.M. Hong, J.W. Jung, J.H. Shim, J.H. Oh, D.W. Cho, 3D printing of composite tissue with complex shape applied to ear regeneration, Biofabrication 6 (2) (2014 Jun), 024103.
[179] B.E.M. Brand-Saberi, T. Schäfer, Trachea: anatomy and physiology, Thorac. Surg. Clin. 24 (1) (2014 Feb) 1–5.
[180] D.M. Hyde, Q. Hamid, C.G. Irvin, Anatomy, pathology, and physiology of the tracheobronchial tree: emphasis on the distal airways, J. Allergy Clin. Immunol. 124 (6 Suppl) (2009 Dec) S72–S77.
[181] B.F. Adams, G.J. Berry, X. Huang, R. Shorthouse, T. Brazelton, R.E. Morris, Immunosuppressive therapies for the prevention and treatment of obliterative airway disease in heterotopic rat trachea allografts, Transplantation 69 (11) (2000 Jun 15) 2260–2266.
[182] B. Gao, H. Jing, M. Gao, S. Wang, W. Fu, X. Zhang, X. He, J. Zheng, Long-segmental tracheal reconstruction in rabbits with pedicled Tissue-engineered trachea based on a 3D-printed scaffold, Acta Biomater. 97 (2019 Oct 1) 177–186.
[183] J. Tao, S. Zhu, N. Zhou, Y. Wang, H. Wan, L. Zhang, Y. Tang, Y. Pan, Y. Yang, J. Zhang, R. Liu, Nanoparticle-stabilized emulsion bioink for digital light processing based 3D bioprinting of porous tissue constructs, Adv. Healthcare Mater. 11 (12) (2022 Jun), e2102810.
[184] H. Hong, Y.B. Seo, D.Y. Kim, J.S. Lee, Y.J. Lee, H. Lee, O. Ajiteru, M.T. Sultan, O. J. Lee, S.H. Kim, C.H. Park, Digital light processing 3D printed silk fibroin hydrogel for cartilage tissue engineering, Biomaterials 232 (2020 Feb), 119679.
[185] S.H. Kim, H. Hong, O. Ajiteru, M.T. Sultan, Y.J. Lee, J.S. Lee, O.J. Lee, H. Lee, H. S. Park, K.Y. Choi, J.S. Lee, H.W. Ju, I.S. Hong, C.H. Park, 3D bioprinted silk fibroin hydrogels for tissue engineering, Nat. Protoc. 16 (12) (2021 Dec) 5484–5532.
[186] J.H. Park, J.Y. Park, I.C. Nam, M. Ahn, J.Y. Lee, S.H. Choi, S.W. Kim, D.W. Cho, A rational tissue engineering strategy based on three-dimensional (3D) printing for extensive circumferential tracheal reconstruction, Biomaterials 185 (2018 Dec) 276–283.
[187] Y. Huo, Y. Xu, X. Wu, E. Gao, A. Zhan, Y. Chen, Y. Zhang, Y. Hua, W. Swieszkowski, Y.S. Zhang, G. Zhou, Functional trachea reconstruction using 3D-bioprinted native-like tissue architecture based on designable tissue-specific bioinks, Adv. Sci. 9 (29) (2022 Oct), e2202181, https://doi.org/10.1002/advs.202202181. Epub 2022 Jul 26. PMID: 35882628; PMCID: PMC9561786.
[188] M.M. De Santis, H.N. Alsafadi, S. Tas, D.A. Bölükbas, S. Prithiviraj, I.A.N. Da Silva, M. Mittendorfer, C. Ota, J. Stegmayr, F. Daoud, M. Königshoff, K. Swärd, J. A. Wood, M. Tassieri, P.E. Bourgine, S. Lindstedt, S. Mohlin, D.E. Wagner, Extracellular-matrix-Reinforced bioinks for 3D bioprinting human tissue, Adv. Mater. 33 (3) (2021 Jan), e2005476.
[189] R. Di Gesù, A.P. Acharya, I. Jacobs, R. Gottardi, 3D printing for tissue engineering in otolaryngology, Connect. Tissue Res. 61 (2) (2020 Mar) 117–136.

[190] E.A. Makris, A.H. Gomoll, K.N. Malizos, J.C. Hu, K.A. Athanasiou, Repair and tissue engineering techniques for articular cartilage, Nat. Rev. Rheumatol. 11 (1) (2015 Jan) 21–34.
[191] D.J. Menger, G.J. Nolst Trenité, Irradiated homologous rib grafts in nasal reconstruction, Arch. Facial Plast. Surg. 12 (2) (2010 Mar-Apr) 114–118.
[192] H.G. Yi, Y.J. Choi, J.W. Jung, J. Jang, T.H. Song, S. Chae, M. Ahn, T.H. Choi, J. W. Rhie, D.W. Cho, Three-dimensional printing of a patient-specific engineered nasal cartilage for augmentative rhinoplasty, J. Tissue Eng. 10 (2019 Jan 16), 2041731418824797.
[193] X. Lan, Y. Liang, M. Vyhlidal, E.J. Erkut, M. Kunze, A. Mulet-Sierra, M. Osswald, K. Ansari, H. Seikaly, Y. Boluk, A.B. Adesida, In vitro maturation and in vivo stability of bioprinted human nasal cartilage, J. Tissue Eng. 13 (2022 Mar 17), 20417314221086368.
[194] S. Roberts, H. Evans, J. Trivedi, J. Menage, Histology and pathology of the human intervertebral disc, J Bone Joint Surg Am 88 (Suppl 2) (2006 Apr) 10–14.
[195] D.H. Heo, D.C. Lee, H.S. Kim, C.K. Park, H. Chung, Clinical results and complications of endoscopic lumbar interbody fusion for lumbar degenerative disease: a meta-analysis, World Neurosurg 145 (2021 Jan) 396–404.
[196] Z. Liu, H. Wang, Z. Yuan, Q. Wei, F. Han, S. Chen, H. Xu, J. Li, J. Wang, Z. Li, Q. Chen, J. Fuh, L. Ding, H. Wang, B. Li, High-resolution 3D printing of angle-ply annulus fibrosus scaffolds for intervertebral disc regeneration, Biofabrication 15 (1) (2022 Dec 15).
[197] B. Sun, M. Lian, Y. Han, X. Mo, W. Jiang, Z. Qiao, K. Dai, A 3D-Bioprinted dual growth factor-releasing intervertebral disc scaffold induces nucleus pulposus and annulus fibrosus reconstruction, Bioact. Mater. 6 (1) (2020 Aug 14) 179–190.
[198] S.L. Ding, X.Y. Zhao, W. Xiong, L.F. Ji, M.X. Jia, Y.Y. Liu, H.T. Guo, F. Qu, W. Cui, Q. Gu, M.Z. Zhang, Cartilage lacuna-inspired microcarriers drive hyaline neocartilage regeneration, Adv. Mater. (2023 Mar 6), e2212114.
[199] L. Kong, G. Yang, J. Yu, Y. Zhou, S. Li, Q. Zheng, B. Zhang, Surgical treatment of intra-articular distal radius fractures with the assistance of three-dimensional printing technique, Medicine (Baltim.) 99 (8) (2020 Feb), e19259.
[200] M.R. Maydanshahi, A. Nazarian, D. Eygendaal, M.H. Ebrahimzadeh, A. R. Kachooei, S.A. Mousavi Shaegh, 3D printing-assisted fabrication of a patient-specific antibacterial radial head prosthesis with high periprosthetic bone preservation, Biomed. Mater. (3) (2021 Mar 5) 16.
[201] G. Zhou, H. Jiang, Z. Yin, Y. Liu, Q. Zhang, C. Zhang, B. Pan, J. Zhou, X. Zhou, H. Sun, D. Li, A. He, Z. Zhang, W. Zhang, W. Liu, Y. Cao, In Vitro regeneration of patient-specific ear-shaped cartilage and its first clinical application for auricular reconstruction, EBioMedicine 28 (2018 Feb) 287–302.
[202] E. Goddard, S. Dodds, Ethics and policy for bioprinting, Methods Mol. Biol. 2140 (2020) 43–64.